THESIS

COMPUTATIONAL FLUID DYNAMICS-BASED MODELING OF METHANE FLOWS AROUND OIL AND GAS EQUIPMENT

Submitted by

Abhinav Anand

Department of Mechanical Engineering

In partial fulfillment of the requirements

For the Degree of Master of Science

Colorado State University

Fort Collins, Colorado

Summer 2025

Master's Committee:

Advisor: Daniel B. Olsen
Co-Advisor: Kira B. Shonkwiler

Dan Zimmerle
Anna Hodshire

ABSTRACT

COMPUTATIONAL FLUID DYNAMICS-BASED MODELING OF METHANE FLOWS AROUND OIL AND GAS EQUIPMENT

Recent studies estimate that emissions from oil and gas (O&G) production facilities contribute between 20 to 50% of the total methane emitted in the US; therefore, quantifying and reducing these emissions is crucial for achieving climate goals. Some methane quantification depends on both measuring methane concentrations and converting these to emissions through a modeling framework. Currently, simple atmospheric dispersion models are primarily used to quantify emissions and concentrations, but these estimates are highly uncertain when quantifying emissions from complex aerodynamic sources, such as oil and gas facilities. This investigation uses a CFD modeling approach, which can account for aerodynamic complexity but has hitherto not been used to model methane concentrations downwind of a methane release of known rate and compared against in-situ measurements. High-time resolution (1 Hz) methane concentration and meteorological data were measured during experiments conducted at Methane Emissions Technology Evaluation Center (METEC) on 21st March and 11th July 2024. The METEC site configuration, measured wind data, and controlled emission rates were used as input for CONVERGE CFD to model downwind methane concentration. The downwind modeling was done between 20-70 meters, each from two different points of release in two separate controlled release experiments— one from a separator and another from a wellhead. In these experiments, we found that the CFD model can predict methane concentrations downwind of the release to a good degree. The fractional bias in maximum modeled concentration was under 32%, and the fractional bias in time-averaged mean methane concentration was under 41%. The model evaluated on multiple metrics to assess its performance in estimating methane concentrations at typical fence-line distances ($\sim$30 m). These results help

to understand external flows and the ability of CFD models to predict downwind concentrations in aerodynamically complex environments.

ACKNOWLEDGEMENTS

I would like to thank Dan Zimmerle, Mechanical Engineering Department and the Energy Institute for initiating, commissioning and supporting this project. I would also like to thank Dr Stuart Riddick for his support throughout my stay at CSU. I would also like to thank Dr Kira B Shonkwiler for ensuring that I followed through with this project to completion. I would like to thank my lab members- Michael Moy, Mercy Mbua, Mercy Ngulat, Elijah Kiplimo, Aashish Upreti, Chiemezie Ilonze for support and discussions. Finally, I would like to thank everyone at METEC who contributed to this project. Last but not least, thanks to my parents who have not seen me in a long time.

DEDICATION

To my parents S S Prasad and Madhumala Sinha.

TABLE OF CONTENTS

LIST OF TABLES

LIST OF FIGURES

Chapter 1

Introduction

1.1 Background

Climate change is one of the most pressing challenges today, with greenhouse gas (GHG) emissions increasing significantly since the mid-19th century [1]. Methane is a potent GHG as its global warming potential is 25 times greater than carbon dioxide [2]. As the largest component of natural gas, methane emissions are particularly significant, and according to the EPA's GHG inventory, one-third of these emissions originate from the oil and gas sector [3]. Therefore, reducing emissions from natural gas production is essential for meeting climate-specific goals. Given the environmental and commercial implications of fugitive emissions, significant attention has been directed toward their identification through continuous emission monitoring (CEM) systems. Continuous emission monitoring systems typically consist of data from low-cost methane sensors and meteorological sensors, which are used in simple atmospheric dispersion models to identify, localise, and quantify emissions. Continuous emission monitoring approaches are particularly beneficial for detecting short-duration, high-emission events, which are characteristic of emissions in the oil and gas sector, since these solutions continuously monitor entire facilities and can identify fugitive emissions faster than existing survey methods [4, 5].

Various types of methane sensors could be employed in these monitoring systems, including metal oxide (MOx), non-dispersive infrared, tunable diode laser absorption spectroscopy (TDLAS), and cavity-based spectroscopic instruments. These sensors vary in price and technology. From the cheapest MOx sensors, with limited sensitivity and costs around $10-20, to cavity-based spectrometers, like ABB's Microportable Greenhouse Gas Analyzer (MGGA) [6] and Picarro's Cavity Ring-Down Spectroscopy [7], which are highly sensitive (ppb level sensitivity) instruments costing $\sim$$50,000. Recent studies have shown that even the lowest cost/precision/accuracy sensors can measure methane concentrations typically associated with fugitive sources very well, close

to ±5% [8–12]. However, the primary limitation in current quantification [13] systems and the widely discussed continuous monitoring solutions [4, 5, 14] lies in the dispersion modeling techniques employed. While dispersion models typically used are well-established and user-friendly for quantifying emissions at fence-lines (∼30 m), they have several limitations. The methods commonly used in this context, such as Gaussian plume (GP) or Gaussian puff models, are significantly limited by assumptions regarding atmospheric conditions, spatial variability, and the complexity of real-world scenarios. Addressing these limitations is essential to enhance the accuracy and effectiveness of emission quantification efforts.

Most dispersion models assume simplified zones of uniform concentration profiles that move with the mean wind direction, using wind profile, local temperature, and other meteorological parameters. Some dispersion models assume a plume shape that spreads as it travels downwind and utilize parameters considering atmospheric conditions and stability. The widely used Gaussian plume model describes the contaminant concentration from a point source as a steady-state plume whose horizontal and vertical spread is modeled as a Gaussian distribution and is under the assumption of a constant wind field. However, this steady-state assumption is often invalid because of changing wind speed and directions, and individual emission estimates using near-source measurements on production sites can be significantly overestimated [15].

To address this shortcoming, the Gaussian puff model was proposed to better accommodate time-varying wind and emission rates. The Gaussian puff model approximates a continuous emission as a series of discrete puffs emitted successively from a point source, with the overall predicted concentration being the sum of the concentration contribution of each puff, with a recent study showing that the Gaussian puff model outperforms the Gaussian plume model [16]. All these methods are variations of one another, generally representing computationally inexpensive modeling approaches. Gaussian models have proven accurate within ±40% for distances less than 1km [17] and are used for long-range concentration estimations, not at fence-line distances typical of oil and gas facilities. Recent studies also highlight significant uncertainties when measurements are taken at typical fence-line distances (∼30 m) [18].

The primary limitation of these simpler approaches is their inability to account for complex aerodynamic environments. Two potential solutions could address this shortcoming, including taking measurements farther from the emission source or employing more computationally intensive modeling techniques. Studies conducted at the METEC facility show that taking measurements farther from the source reduces uncertainty. However, taking this into account may be prohibitively expensive as fence-line methane analysers would have to be more sensitive (TDLAS or optical cavity), and production sites would have to be larger (up to 5 times larger). While dispersion modeling methods are effective in scenarios involving unobstructed flows over flat terrain, computational fluid dynamics (CFD) is believed to offer enhanced capabilities for simulating flows in complex environments, including around obstacles and real-life obstructions. This advancement could lead to more accurate and reliable assessments of methane dispersion.

Computational fluid dynamics addresses the fundamental Navier-Stokes [19] equations across the entire problem domain. These equations, a set of coupled differential equations, describe the relationships among velocity, pressure, temperature, and density of a moving fluid. As second-order equations, they cannot be solved analytically for real-world applications; instead, they are solved numerically. Computational fluid dynamics has not been widely employed to model methane emissions from natural gas production sites due to its computational expense and time-intensive nature, with a single run potentially taking hours or even days to yield results compared to a few minutes for a Gaussian plume model. However, advancements in computational power and the availability of high-performance computing (HPC) facilities present promising opportunities for applying CFD in the oil and gas sector, particularly in modeling methane emissions. This could lead to more accurate and detailed assessments of methane dispersion and its financial and environmental impact.

Computational fluid dynamics could overcome the shortcomings of more straightforward Gaussian approaches as CFD models don't assume a plume shape and are better suited to simulate flows in non-flat terrain and around complex obstructions like oil and gas equipment. Unlike simpler Gaussian models, a CFD model can better account for spatial and temporal variation in the local

wind speed. Wind data are input with variation in three dimensions at a frequency of 1 Hz, which is difficult for simple Gaussian models. A few studies have looked at the ability of dispersion models and CFD to simulate plumes, with findings that CFD is more capable around obstruction and terrain [20–22]. These findings reinforce earlier results that found dispersion models poor at calculating the flow over obstacles or with spatial/temporal variations in weather conditions [23].

1.2 Existing Work

Computational fluid dynamics models are much more complex than the Gaussian plume models, however they are used now to simulate atmospheric dispersion. This is attributed not only to advancements in computational power but better availability of computational resources like HPC facilities. Computational fluid dynamics models have been used widely to study CO_2 dispersion in outdoor and indoor environments. Mazzoldi et al. [24] compared the performance of a numerical CFD model Fluidyn-PANACHE [25] and Gaussian model ALOHA [26] with Prairie Grass [27] and Kit Fox field experiments [28] showing that a CFD model performs well inside the limits of acceptability for atmospheric dispersion software and much better than Gaussian models. Schleder and Martins [29] used a CFD tool FLACS to investigate its performance for cloud dispersion of toxic/flammable substances. The FLACS model solves Reynolds Averaged Navier-Stokes (RANS) equations based on the k-ϵ turbulence model. The study found that the software could estimate peak concentration well with acceptable statistical performance. Toja and Silva [30] used CFD simulations of CO_2 dispersion from a natural gas-fueled thermal power plant in an urban environment using a self-customized version of the open-source and open-access software OpenFOAM [31]. The fluid flow (wind) is initially solved using the steady RANS equations, and gas transport and diffusion are solved using the unsteady convection-diffusion equation. The model results were then compared with experimental measurements of column-averaged dry-air mole fraction on the site, obtaining a good agreement. They also recommended the optimum turbulent Schmidt number for the application. Tan et al. [32] carried out wind tunnel experiment and CFD simulations to study dispersion of CO_2 plume in street canyons. The CFD software ANSYS-Fluent was used to carry

out the numerical simulation using Shear Stress Transport (SST) k-ω turbulence model agreeing well with the experimental data. Wareing et al. [33] studied near-field CO_2 dispersion using CFD models employing the RANS turbulence modeling with adaptive mesh refinement. Wen et al. [34] studied far-field dispersion modeling of CO_2 release from a vertical vent and from a horizontal 'shock tube' test rig. In another study by Wen et al. [35] a dedicated CFD solver was developed specifically for the dispersion of CO_2 from pipeline releases. Liu et al. [36] validated CFD models for decompression and dispersion of CO_2 releases from pipelines. Simulations were carried out using the commercial CFD software ANSYS Fluent [37], which applies the Finite Volume Method to discretise the governing differential equations of fluid flow, including the Reynolds-Averaged Navier–Stokes (RANS) equations. It was found that CFD models performed well in predicting the time-varying CO_2 concentration pattern, but Phast UDM, a dispersion model, tended to under-predict the concentration levels. Joshi et al. [38] also used ANSYS Fluent to simulate far-field CO_2 dispersion and found it to be in good agreement with measurements up to 100 m downwind.

All the above studies, although they validate the application of CFD models as atmospheric dispersion tools they were used to study gaseous dispersion from the viewpoint of toxicity/flammability. Although both CO_2 and CH_4 are GHGs, not many comprehensive studies have been done on modeling methane using CFD. The aforementioned studies simulate CO_2 releases from a pipeline failure or accidental releases at much larger rate than from leaks at an O&G facility on a day-to-day basis (0.09-6.4 kg CH_4/h, release rates at METEC). In addition, the models were not validated against CO_2 release experiments due to scarcity of publicly available datasets. Many of the studies were validated against experiments conducted in the past decades done by separate research entities [24, 38] or scaled down wind tunnel experiments [32, 33]. Although scaling is a common practice in CFD, this work is oriented to real scale applications where real magnitudes are represented. Mazzoldi et al. [24] evaluated results from a CFD and a Gaussian plume model against the Prairie Grass field experiments conducted between 50-800 meters [27]. However, our study is limited to under 100 m from the release point. Toja-Silva et al. [30] performed a one to one CFD and Gaussian plume evaluation against the column-averaged dry-air mole fraction of CO_2.

However, this was done at 500 m from the release point of a thermal power plant chimney; far too distant from our interest in our study where we focus on fence-line measurement and modeling. Liu et al. [36] validated CFD model—ANSYS Fluent for dispersion of CO_2 release from pipeline using RANS equations between 5-80 m with no obstruction for "liquid" and "supercritical" CO_2 releases which involved phase conversion and inclusion of *Equation of States* for non-ideal gas behavior. Joshi et al. [38] also studied the near-field dispersion of supercritical CO_2 within 100 m from a pipeline rupture and evaluated against experiments conducted by the British O&G company BP. Wen et al. [34] studied the release and dispersion of CO_2 downwind of a release with self-conducted experiments between 20-100 m however without any equipment/obstruction in the simulation domain. Yet, the study gives a good idea of CFD's ability to model atmospheric dispersion. As far as we know, there are not many full-scale, real-world applications of CFD with known controlled methane releases at an oil and gas-like facility for short distances near fence-line.

1.3 Thesis Overview

This work uses a CFD model (CONVERGE CFD, section 2.5) to quantify downwind methane concentrations at the range of fence-line distances ($\sim$ 30 m), assess its model performance metrics and determine if there is any correlation between model performance and downwind distance. Specifically, the study's objective is to 1. use a CFD tool to model methane released at a known rate from a known position and calculate downwind methane concentration; 2. compare the modeled and measured concentrations to evaluate model performance; 3. investigate how model performance is affected by the size of the aerodynamic obstruction, and finally, 4. compare the CFD model results with equivalent Gaussian plume model results to see if CFD improves over existing simpler models.

To our knowledge, this is the first time a CFD model has been used to calculate concentrations downwind of a methane source at an O&G-like facility and evaluate them through measurement. The next chapter discusses the methods used to complete the above objectives and test the experiment's hypothesis.

Chapter 2

Data & Methods

2.1 Controlled Methane Release Experiment

Controlled methane release experiments were conducted at Colorado State University's Methane Emission Technology Evaluation Center (METEC) in Fort Collins [39], ∼60 miles north of Denver, Colorado. Methane Emission Technology Evaluation Center is a unique test and research facility that was designed to test the efficacy of leak detection and quantification (LDAQ) technologies, field demonstrations, hands-on LDAQ equipment training, and protocol/best practices development. The METEC facility simulates layout of real-world oil and gas facilities using decommissioned equipment and allows enterprises/researchers to test how their LDAQ methods operate in realistic field conditions using emissions sources of known size, duration and gas composition [13, 40].

The METEC facility has a flat terrain covered with grass and O&G equipment across the facility on 7 pads. There are above-ground emissions from oil and gas equipment (Pads 1 to 6; Figure 2.1) and underground emissions from pipeline leaks (Pad 7; Figure 2.1). Our study used only above-ground emission points in pads 4 and 5 (Figure 2.1). Gas is delivered to emission points via small-diameter tubing, and the emission points on the equipment are engineered such that the size and duration of the fugitive emissions are realistic. It is furnished with inactive surface equipment units (e.g., wellheads, separators, tanks etc.) intentionally fitted with points concealed at commonly observed leak sources such as valve packing, flanges, fittings, etc. At the time of the experiments, METEC had approximately 200 above-ground release points, all remotely controlled, from seven pads.

In our study, we performed 2 sets of experiments. The first set of testing was conducted exclusively on pad 5 (Figure 1) on 21st March 2024 between 9-11 AM—controlled release (steady plume) of 1.3 kg CH_4/h from a separator. The second experiment was conducted on 11th July

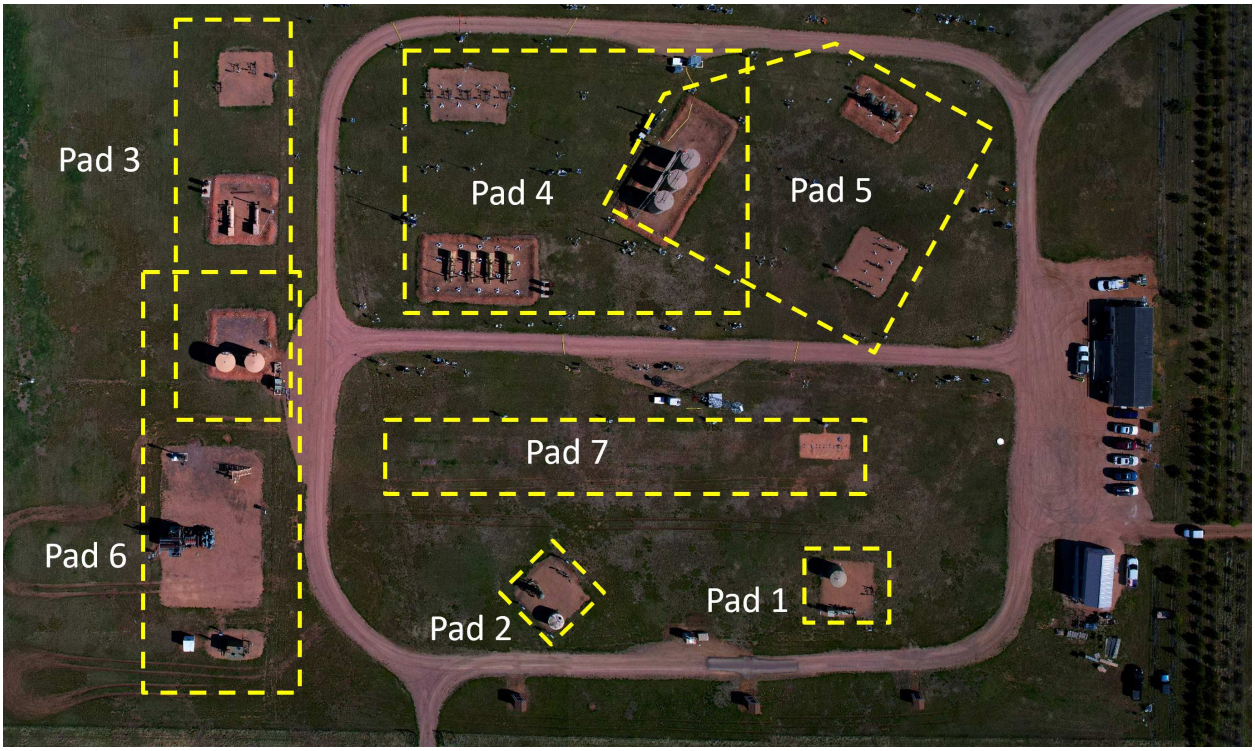

Figure 2.1: A top view of the METEC facility at the time operated CSU Energy Institute, Fort Collins; provided by METEC. North is perpendicular to the top pointing upward.

2024 between 1-3 PM on pad 4 (Figure 1) from a controlled release (steady plume) of 2.6 kg CH_4/h from a wellhead. The equipment on pad 4 and pad 5 have different aerodynamic complexity to methane flow, with different release heights. This is discussed in the sections later. Methane measurements were done at 4 distances from the release point on both days. In both these experiments, there was a single point emission source and a single measurement point with no obstructions between the source and measurement points other than obstructions caused by the O&G equipment itself. All the samples were 4-6 minutes long. Compressed natural gas was used for emissions; its composition was determined using gas chromatography.

2.2 Methane Measurements

Methane concentration measurements at the METEC facility were conducted using a Micro-portable Greenhouse Gas Analyzer (MGGA). The MGGA is a cavity-based spectroscopy instrument based on Off-Axis Integrated Cavity Output Spectroscopy (OA-ICOS) technology by ABB

Technology (Zürich, Switzerland) [41]. The MGGA can measure methane concentration at the rate of 1 to 10 Hz with ppb level sensitivity. The reference concentration data for this work were measured at 1 Hz. The background/ambient methane was established through reference measurements. The calibrated MGGA sensor was set-up in the open when no release was taking place to measure ambient methane concentrations. The background/ambient methane concentration without any methane release in the atmosphere was established to be $\sim$1.8 ppm. The value was verified over multiple measurements in ambient conditions.

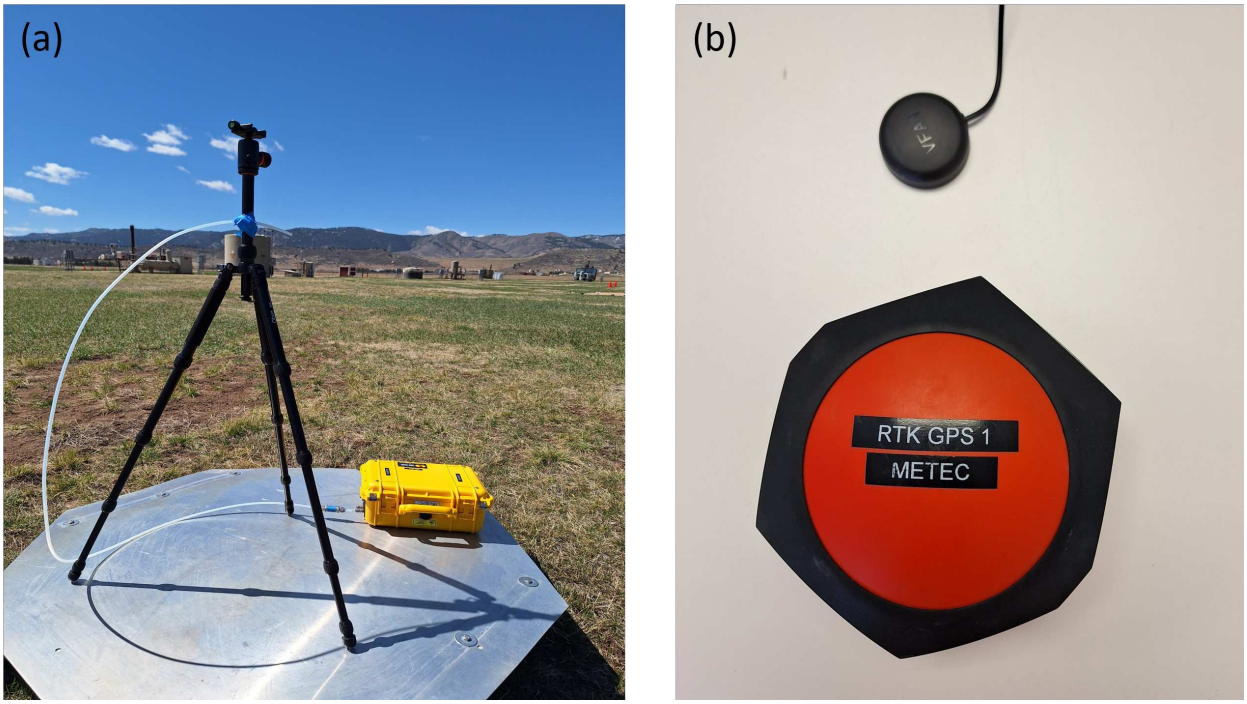

Figure 2.2: Instrument set-up to carry out methane measurements at METEC. (a) MGGA sensor along with a stand and a tubing set up on a tripod. (b) Two different GPS sensors to mark the MGGA location downwind of the release.

The methane measurements were made in a transect downwind or near-downwind of the emission point. Methane analyzers were used to measure dry mole mixing ratios downwind of the controlled release using an inlet to the analyzer 1 meter above the ground. A Global Positioning Sensor (GPS) marker was used alongside the MGGA analyser to note the exact location of the measurement. The instrument setup during field experiments can be found in Figure 2.2. The

samples were collected over a period, typically an hour. This allowed us to collect 4 samples from a single controlled release, each over 4–6 minutes. Figure 2.3 below shows the emission source and sensor location for the 8 samples used in this study.

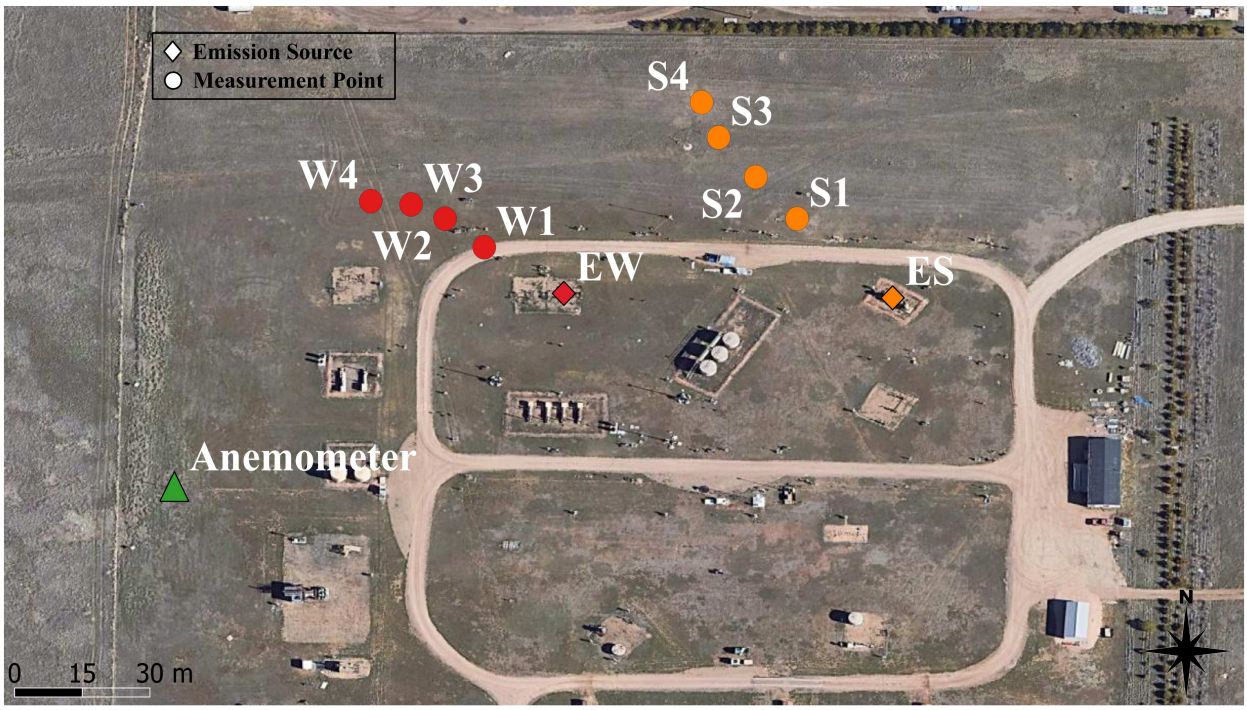

Figure 2.3: Schematic of the emission source and sensor location at METEC for the controlled release experiments. W1 to W4 are measurements made from wellhead emissions, and S1 to S4 are measurements made from separator emissions. Anemometer is shown in green. North is perpendicular to the top pointing upward.

2.3 Meteorological Data

One hertz meteorological data was measured using an R. M. Young 3D sonic anemometer (Traverse City, MI, USA) [42] and consists of sonic temperature, pressure, relative humidity, and wind speed in three directions. The mean wind speed on the 21st of March 2024, during the data collection period was 2 m/s, between 0.6 and 3.4 m/s, and 3 m/s on the 11th of July 2024, between 0.3-5.8 m/s. During both measurements, southeast wind blew varying between 120 and 150 degrees from the north (Figure 2.4).

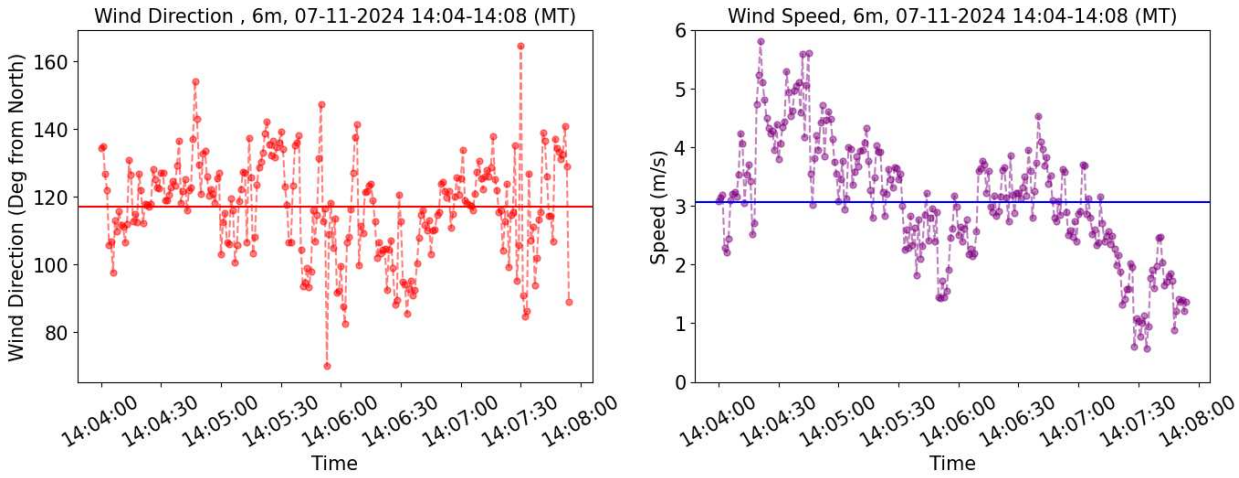

Figure 2.4: Wind direction and wind speed over a period of 4 minutes on July 11th, 2024, during field data collection.

2.4 Wind Modeling

The wind data collected at METEC was used to model wind speed with height between ground level to 15 m above the ground level using reference wind speed (u*, m/s) at the height of 6 meters, roughness length (z_0, m) and von Karman constant (k), as shown in Equation 2.1 [43]. The roughness length (z_0) varies with surface, the surface roughness length in this study is based on assumed roughness ($\sim$ 5 cm) upstream of the releases at METEC, and the von Karman constant is a dimensionless constant (0.4). The same equation is used in Wen et al. to model wind for CFD modeling [34].

$$\mathrm{u(z)} = \frac{u^*}{k} \log(\frac{z}{z_0}) \tag{2.1}$$

2.5 CFD Modeling

Computational modeling of the methane flow was done in CONVERGE CFD (Convergent Science, Madison, Wisconsin) [44]. We opted for RANS turbulence modeling. It is the most common and widespread approach [24, 33, 34, 45]. Reynolds-Average Navier-Stokes simulations require the least computational resources- while still maintaining a good level of accuracy [46] when compared to detached numerical simulation (DNS) and large eddy simulation (LES), the

other turbulence options in the model. The best results can be obtained using DNS since it does not have many modeling assumptions. However, DNS is computationally very expensive due to its very fine spatial and temporal resolution. Large eddy simulation falls in the middle, and has been used in some studies, yet still at larger computational cost than RANS [47]. Apart from the computational expense of LES for full-scale environments, there is not enough evidence to justify the use of LES models for fence line emission modeling. Most of the experiments used to validate LES simulations were done in wind tunnels or near-ideal conditions [48]. A study by Patnaik et al. [49] reported some degree of reliable prediction using LES simulation in a real site but with great uncertainty. Therefore, the benefits of using LES instead of RANS in simulating outdoor environments are not very much proven yet. In interest of computational expense, we use RANS for our study. With RANS, flow variables (e.g., velocity) are decomposed into an ensemble mean and a fluctuating term [50]. For the RANS simulations in this work, boundary conditions (BC) were set for emission inflow, outflow and at other boundaries, i.e., pipeline, equipment (tank, separators, pads), and ground (Figure 2.5). The BC were usually either (1) no slip solid surfaces, (2) wind inflow or outflow, (3) a passive outflow condition at ambient pressure. More on the model setup can be found in Table 2.1.

Table 2.1: Physics options used with CONVERGE CFD simulations.

	Option	Physics
1	Navier-Stokes Solver Scheme	Pressure Implicit with Splitting of Operator/(PISO)
2	Navier-Stokes Solver Type	Density-based
3	Turbulence Model	RANS
4	Heat Transfer Model	O'Rourke and Amsden
5	Near-wall Treatment	Standard wall function

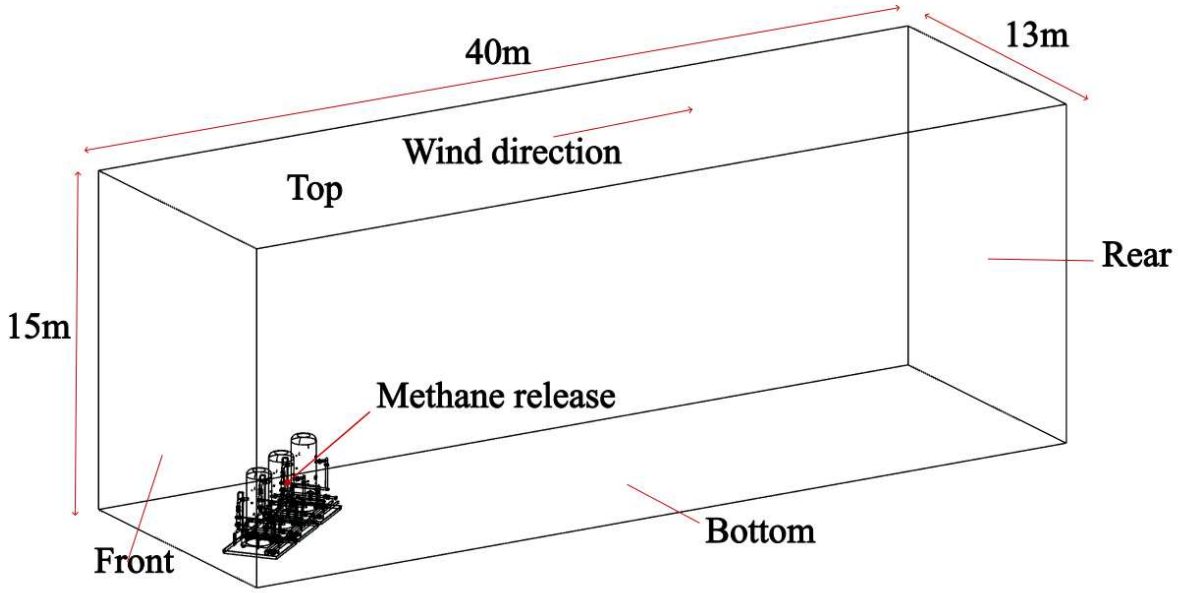

Figure 2.5: Model domain for CONVERGE CFD simulations for the separator experiment.

2.5.1 Meshing

Meshing in CFD is the process of generating a grid of elements to discretize the model domain; the resulting structure is called a mesh. It involves dividing complex geometries into recognizable volumes called elements. CONVERGE CFD requires equipment geometry as input, and computer aided design (CAD) models were generated for METEC equipment using Fusion360 (Autodesk Inc, USA) [51]. Since CONVERGE uses STL files as geometry input, CAD geometry files were converted to STL and imported to CONVERGE. It is advantageous as CONVERGE CFD automatically generates structured orthogonal grids during the runtime depending on the defined inputs to fixed embedding, adaptive mesh refinement (AMR), and grid scaling, which eliminates the manual control of grid size [52, 53]. Fixed embedding is to refine the grids at specific locations in the domain where a finer resolution is critical to the accuracy of the solution (Figure 2.6). Grid scaling refers to changing the base grid size between desired events during a simulation, which reduces the runtime by coarsening the grids during noncritical simulations and can help capture a critical flow phenomenon by refining the grids at specific times. The AMR input refines the mesh based on fluctuating and moving boundary conditions such as velocity and temperature.

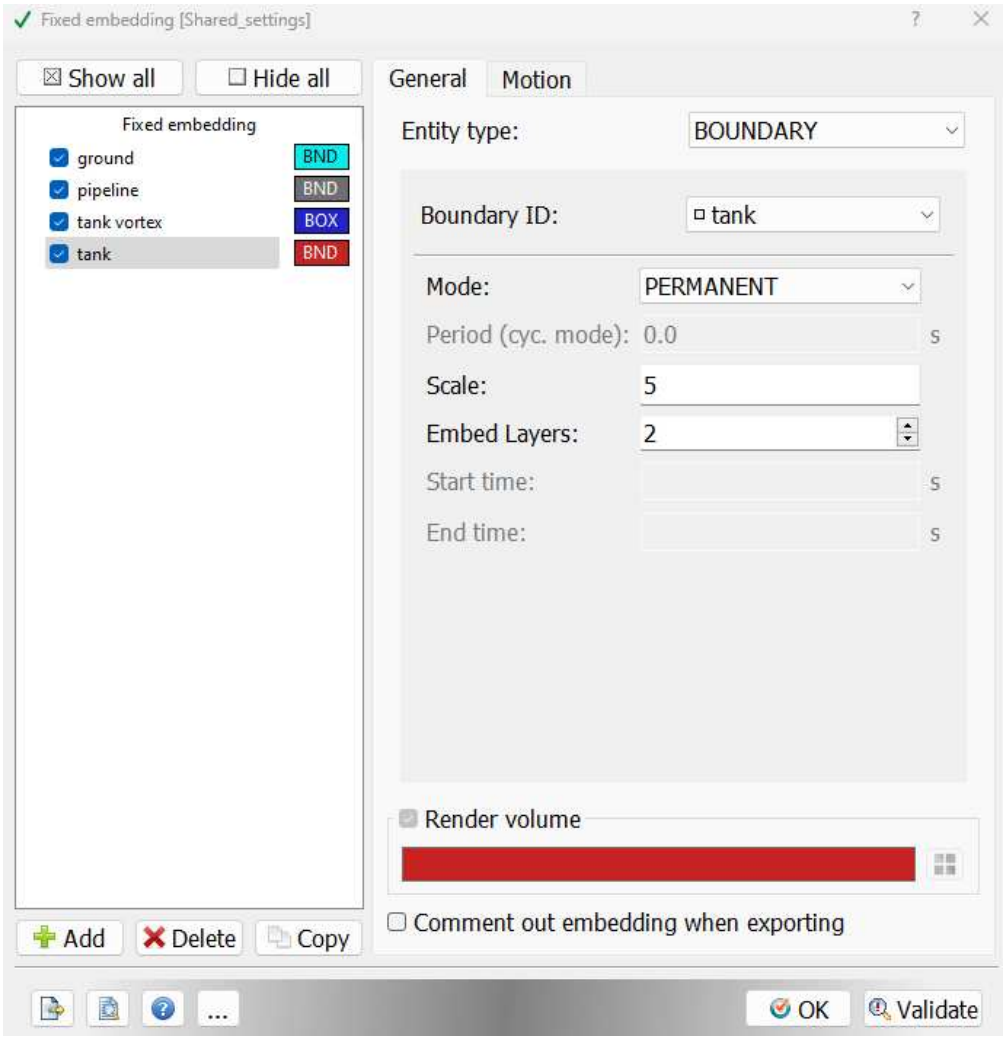

Figure 2.6: Fixed embedding settings for ground, pipeline, tank and tank vortex in model setup.

2.5.2 Monitoring Points

Monitoring points in 3-dimensional space were set up in the CFD to record simulated methane concentrations [24, 34, 36]. Monitoring points are the specific points in the model domain corresponding to the measurement point from the field studies. Five monitoring points were created a meter apart at to capture the uncertainty in the sensor location at the measurement point (Figure 2.7). The final concentration is calculated as the mean at the 5 points. In addition to the monitoring points at 1-meter height above the ground, more points were marked at 2 m and 3 m in the model to understand the concentration gradient with height. For each CONVERGE simulation, 15 monitoring points were set up.

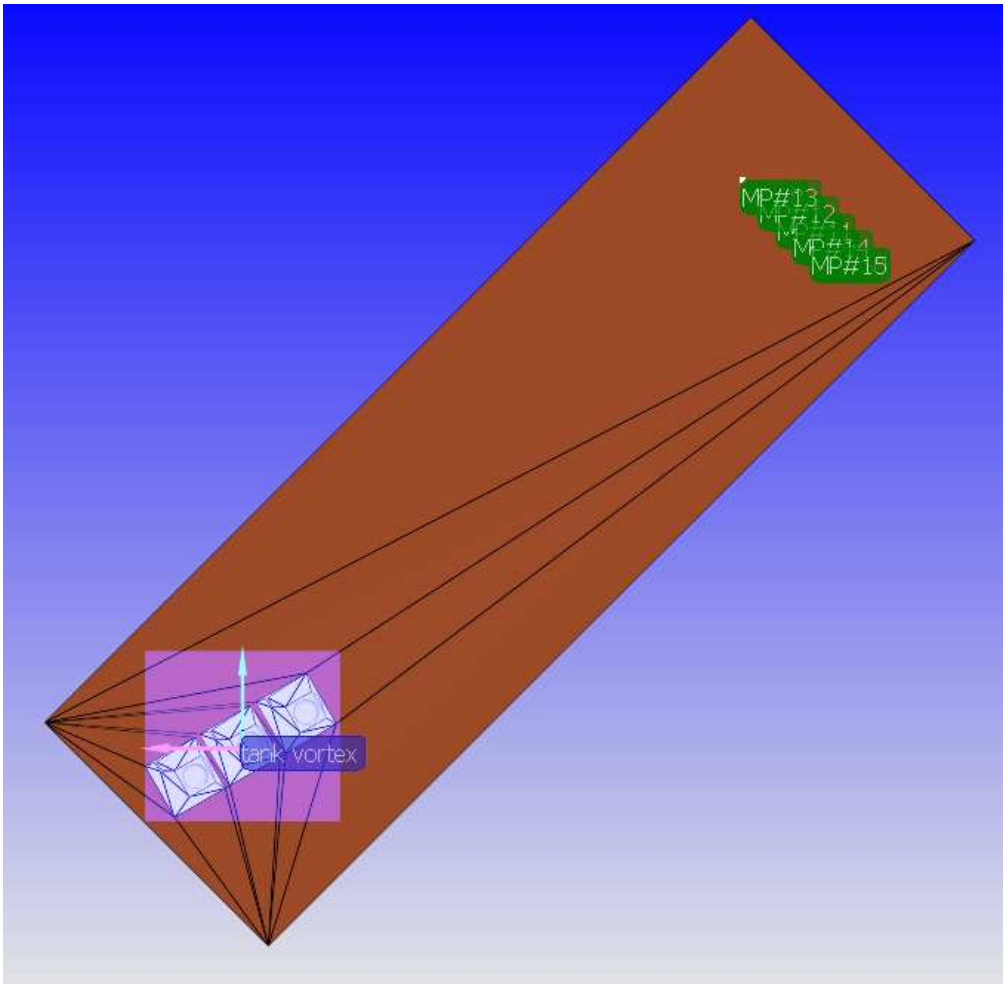

Figure 2.7: Monitoring points marked in green in the model domain downwind of the methane release.

2.6 Gaussian Plume Modeling

The CFD model results were also evaluated against results from a Gaussian plume model. The Gaussian plume model used in the study is described below.

The Gaussian plume model describes the contaminant concentration from a point source as a steady state plume whose horizontal and vertical spread are modeled as Gaussian distributions (Equation 2.2). The gas concentration (C, $\mu g/m^3$) is measured at a distance downwind from the point source at a distance (x, m), lateral distance laterally from the plume centerline (y, m), and height above the ground level (z, m). Here, H_o (m) is the source height, the emission rate is Q (kg/s) and wind speed is u (m/s).

$$\text{C(x,y,z)} = \frac{Q}{2\pi u \sigma_y \sigma_z} \exp(\frac{-y^2}{2\sigma_y^2})[\exp(-\frac{(z-H_o)^2}{2\sigma_z^2}) + \exp(-\frac{(z+H_o)^2}{2\sigma_z^2})] \tag{2.2}$$

Where $\sigma_y = \sigma_y(x)$ and $\sigma_z = \sigma_z(x)$ are dispersion parameters that control the width of the plume in the y and z directions, respectively, and are functions of downwind distance x only. The dispersion parameters are typically computed using the empirical equations given below:

$$\sigma_z = ax^b \tag{2.3}$$

$$\sigma_y = 465.11628x \tan\theta \tag{2.4}$$

$$\theta = 0.017453293[c - d\log(x)] \tag{2.5}$$

Where the units of σ_y and σ_z are [m] and the units of x are [km]. The a, b, c, d parameter values in (Equation 2.3-2.5) are a function of the Pasquill-Gifford atmospheric stability class and can be obtained from the PGSC lookup table (Appendix A).

2.7 Model Evaluation Metrics

The evaluation of modeled methane concentration in this research was done on multiple metrics based on previous studies by Weil et al. [54], Hanna et al. [55] and summarized in Chang and

Hanna [56]. These studies are now nearly 3 decades old however the metrics have been used in many recent papers [30, 34, 35, 38]. The fractional bias (FB) (Equation 2.6) and geometric mean bias (MG) (Equation 2.7) measure systematic bias, whereas normalized geometric variance (VG) (Equation 2.8) and mean square error (NMSE) (Equation 2.9) measure random scatter. There is not a single performance measure that is universally applicable to all situations, and a balanced approach is required to look at a number of performance measures. For dispersion modeling where concentrations can easily vary by several orders of magnitude, MG and VG are preferred over FB and NMSE. However, MG and VG may be strongly influenced by very low values, and are undefined for zero values. The Fraction of two of the Observations (FAC2) (Equation 2.10) is probably the most robust performance measure, because it is not overly influenced by either low or high outliers. A perfect model would have MG, VG and FAC2 = 1; FB and NMSE = 0. These values are generally not attainable in studies, however, minimum acceptable performance measures are summarized by Chang and Hanna [56]— the fraction of predictions within a factor of two from observations i.e., about 50% (i.e., FAC2 > 0.5); the mean bias within ±30% of the mean (i.e., -0.3 < FB < 0.3 or 0.7 < MG < 1.3); and the random scatter about a factor of two of the mean (i.e., NMSE < 4 or VG < 1.6). The absolute mentioned in the study later for FB is the modulus of FB i.e., the positive value of the number.

$$\text{Fractional Bias (FB)} = \frac{Mod - Obs}{2 * (Mod + Obs)} \tag{2.6}$$

$$\text{Geometric Mean Bias (MG)} = \exp(\overline{\log(Obs_i)} - \overline{\log(Mod_i)}) \tag{2.7}$$

$$\text{Geometric Variance (VG)} = \exp(\overline{(\log(Obs_i) - \log(Mod_i))^2}) \tag{2.8}$$

$$\text{Normalized Mean Square Error (NMSE)} = \frac{\overline{(Mod - Obs)^2}}{\overline{Mod} * \overline{Obs}} \tag{2.9}$$

$$\text{Fraction of two of the Observations (FAC2)} = \text{Fraction of data that satisfy } 0.5 \leq \frac{Mod}{Obs} \leq 2 \tag{2.10}$$

These performance measures are not exhaustive, hence model evaluation has also been done on additional metrics not discussed in these studies. To estimate how the model performs over the duration of the simulation at each distance, we calculated the normalised mean bias (NMB) (Equation 2.11) [57]. We calculate the correlation coefficient (R) (Equation 2.12). Though it is sensitive to outliers it tells us how strongly the model-simulated concentrations are related to the observations. We also calculate the root mean square error (RMSE) (Equation 2.13), which tells us how the modeled values deviate from the observed values, on average. Finally, the similarity between the modeled and observed concentration distributions is calculated using an overlap coefficient. The model and observed concentrations were binned in 50 equal bins of 2 ppm size, and then the overlapping area between the two distributions was calculated to give the overlapping coefficient (Equation 2.14).

$$\text{Normalised Mean Bias (NMB)} = \frac{\sum_{i=1}^{n}(Mod_i - Obs_i)}{\sum_{i=1}^{n} Obs_i} \tag{2.11}$$

$$\text{Correlation Coefficient (R)} = \frac{\sum_{i=1}^{n}(Mod_i - \overline{Mod})(Obs_i - \overline{Obs})}{\sqrt{\sum_{i=1}^{n}(Mod_i - \overline{Mod})^2 \sum_{i=1}^{n}(Obs_i - \overline{Obs})^2}} \tag{2.12}$$

$$\text{Root Mean Squared Error (RMSE)} = \sqrt{\sum_{i=1}^{n} \frac{(Mod_i - Obs_i)^2}{N}} \tag{2.13}$$

$$\text{Overlap Coefficient (OC)} = \frac{\text{Intersection of area under the curve of the two distributions}}{\text{Union of area under the curve of the two distributions}} \tag{2.14}$$

2.8 Limitations and Scope of Study

Results from this study could be helpful to understand the usefulness of CONVERGE CFD to model methane concentrations. However, the study applies to the METEC facility, where pads 4 and 5 are simplified onshore production facilities, and therefore, the results are unlikely to be directly applicable to more or less aerodynamically complex midstream or offshore facilities.

Firstly, there are limitations to the CFD simulations we did for our study. The limitations of the CFD simulations are as follows:

- 1. Pre-existing model physics and suggested parameters (e.g. Schmidt and Prandtl number) were used in all our simulations; the effects of these parameters on results were not studied in our work.

- 2. Furthermore, the mesh was kept coarse to keep the computational time within 24 hours on high performance computing clusters (1 node with 256 GB Memory, 64 CPU cores). The base grid size for the simulations varied between 1-2 m with grid refinement near boundaries-emission source, ground, equipment vortex etc. Typically, a finer mesh can provide better simulation results and model convergence but increased simulation time.

Secondly, wind modeling (section 2.4) was done assuming neutral conditions with z_o of 5 cm, around the METEC facility. The surface roughness length (z_0) in this study is based on assumed roughness upstream of the releases at METEC, hence equipment height was not considered for wind modeling. This could affect the modeled wind speed and turbulence, hence, the CFD modeling results. If a CFD model does not satisfactorily account for larger ranges of atmospheric eddies, it may therefore under-predict turbulence levels [56].

Finally, this study assesses and compares the ability of CFD tools to model external methane flows downwind of a release point. Therefore, subsequent post-processing and detailed performance analysis focusing on the impact of variables (such as underlying model physics, physical parameter values, sensor placement, types of sensors, characteristics of emission points, meteorological conditions, and additional relevant factors) are needed later in future studies [24,36,47,56].

Chapter 3

Results and Discussion

3.1 Wellhead Experiment

The wellheads are situated on pad 4 at the northwest end of the METEC facility (Figure 2.1). There are 5 wellheads next to one another from east to west at a separation of 1.5 meters, and the methane source is located on the 2^{nd} wellhead from the east. The emission source is at a height of 1.5 meters from the ground, and the wellhead structure is less complex than other equipment at the facility. Four measurements were taken downwind of the wellhead, northwest from the source at 22, 33, 43 and 50 meters.

3.1.1 Metrics of Performance: Modeled (CFD) vs Measured Methane Concentrations

The maximum concentration in the observations decreased with increasing distance, with the highest value of 74 ppm observed at 22 m and the lowest concentration measurement of 15 ppm at 50 m. The modeled methane concentrations from these experiments varied between the background concentration ($\sim$1.8 ppm) and 74 ppm (Figure 3.1). The maximum modeled concentration at 22 m distance was 58 ppm, and the maximum modeled methane concentration at 50 m was 29 ppm. The modeled mean concentration across the wellhead experiment at these 4 distances was 4.6 ppm against the observed mean of 3.6 ppm, an overestimation of 28%.

The modeled methane concentrations are first evaluated on the metrics suggested by Hanna et al. [55] and Chang and Hanna [45] and has been used for several studies to evaluate atmospheric dispersion models [24, 34, 58]. The suggested FAC2 values of 50% or more is a good indicator of the model performance, and all the modeled concentrations at all the distances in the wellhead experiment perform well with FAC2 values as high as 0.8 (Table 3.1). The suggested range for MG is between 0.7 and 1.3. The values for this experiment stayed between 0.65 and 0.9, suggesting

the mean bias is within ±30% of the mean. The NMSE is less than 4 however the VG values are higher than the suggested value of 1.6 at two distances, which show a deviation from the range of acceptability. However, the FB in modeled mean and maximum concentration at the two distances are within ±40% (Tables 3.2 and 3.3).

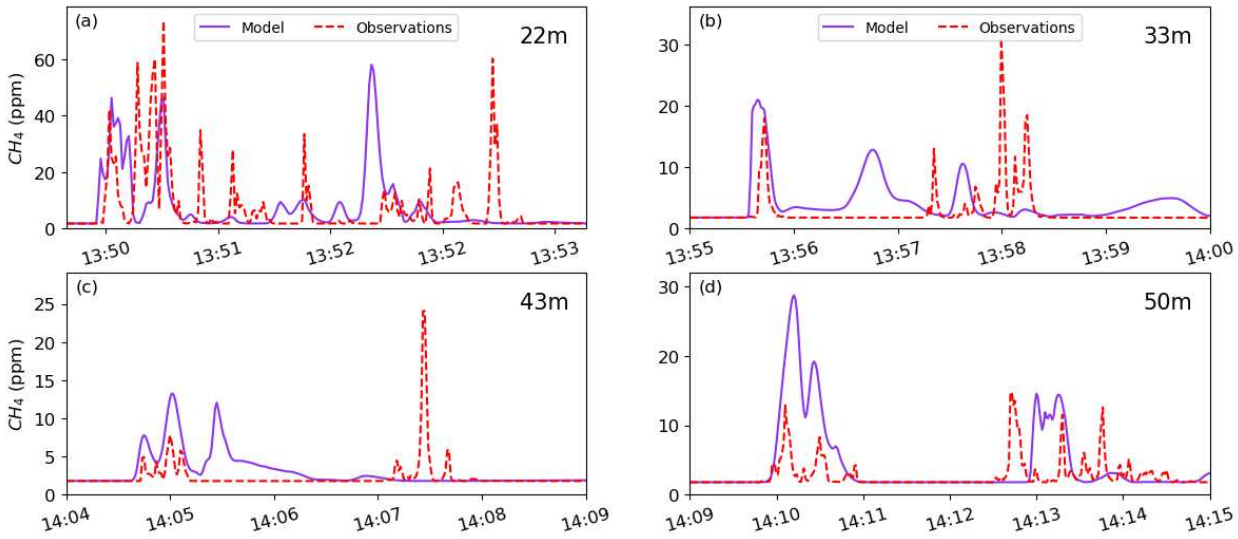

Figure 3.1: Modeled methane concentration plotted against observations for release from the wellhead on 11th July 2024. The y-axis shows the methane concentration with time displayed in hours and minutes (also, y-axes have different bounds in the plots a-d).

Table 3.1: FAC2, MG, VG and NMSE for each experiment when evaluated against observed concentration for the wellhead experiment.

Distance (m)	FAC2	MG	VG	NMSE
22	0.58	0.90	3.91	3.26
33	0.60	0.65	2.07	1.80
43	0.80	0.81	1.42	1.27
50	0.75	0.85	1.81	1.40

Looking at some other metrics, the NMB value for modeled concentrations at 33 m was the lowest of nearly zero, and the value goes up to 0.55 at 50 m, while the NMB values were 0.01 at

Table 3.2: Fractional bias in maximum modeled concentration (CFD) for the wellhead experiment.

Distance (m)	Max Modeled Concentration (ppm)	Max Observed Concentration (ppm)	Fractional Bias (%)
22	58.08	73.58	-24
33	21.02	31.18	-38
43	13.25	24.07	-58
50	28.75	14.7	64

Table 3.3: Fractional bias in time-averaged modeled (CFD) concentration for the wellhead experiment.

Distance (m)	Mean Modeled Concentration (ppm)	Mean Observed Concentration (ppm)	Fractional Bias (%)
22	7.62	7.52	2
33	4.24	2.82	40
43	3.01	2.34	26
50	4.36	2.82	42

22 m and 0.28 at 43 m (Table 3.4). The RMSE values vary between 7-13 ppm for the modeled concentrations. The overlap coefficient characterizes similarity between two populations. The values were high; i.e., 0.72, 0.76 and 0.81 at 22 m, 43 m and 50 m, respectively, with 0.34 at 33 m (Table 3.4). The R-values stayed between 0.26 and 0.29 (Table 3.4) suggesting a weak linear relation.

Table 3.4: NMB, R-value, RMSE and overlap coefficient for each experiment when evaluated against observed concentration for the wellhead experiment.

Distance (m)	NMB	R-value	RMSE (ppm)	Overlap coefficient
22	0.01	0.26	13.67	0.72
33	0	0.26	9.6	0.34
43	0.28	0.28	8.38	0.76
50	0.55	0.27	7.17	0.81

3.2 Separator Experiment

The separators are bigger and more complex aerodynamic obstructions situated on pad 5 of the METEC facility (Figure 2.1). There are three separators next to each other and the emission point is 1.7 meters from the ground, located between two separators. Methane measurement were taken at 30 m, 45 m, 60 m and 70 m northwest of the emission source.

3.2.1 Metrics of Performance: Modeled (CFD) vs Measured Methane Concentrations

Similar to the evaluation for the wellhead experiments, the modeled methane concentrations are evaluated on the metrics suggested by Hanna et al. [55] and Chang and Hanna [45]. Later we also use some additional metrics to evaluate model performance.

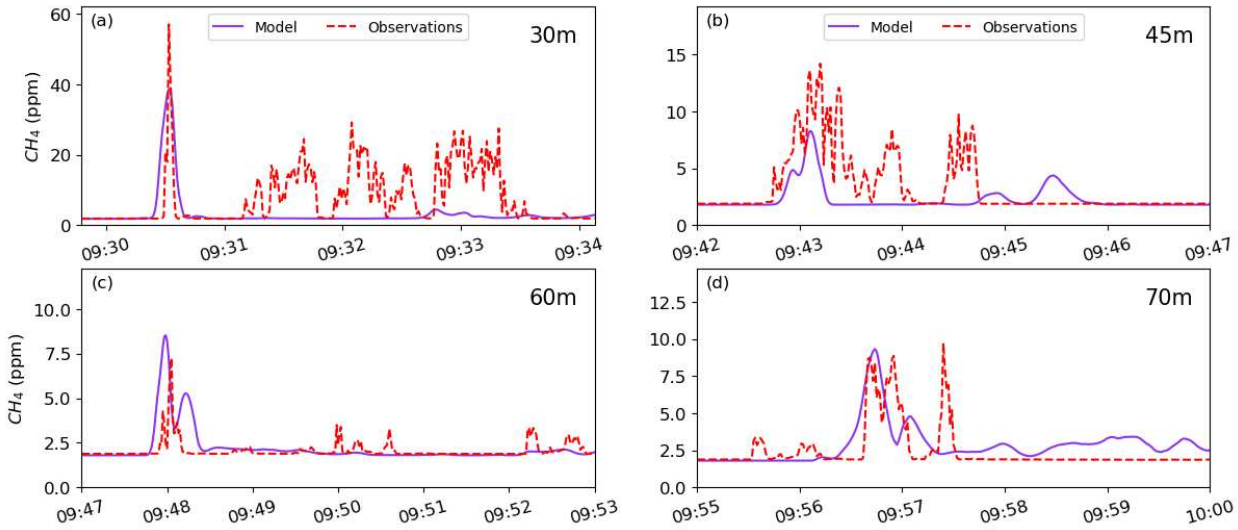

Figure 3.2: Modeled methane concentration plotted against observations for release from the separator on March 21st 2024. The y-axis shows the methane concentration with time displayed in hours and minutes (also, y-axes have different bounds in the plots a-d).

At first, we look at Figure 3.2 to determine the model minima and maxima. The modeled methane concentration peaked at 30 m with a maximum of 39 ppm against the observed concentration of 57 ppm. The modeled and observed methane concentrations decreased with increasing

distance. The time-averaged modeled mean concentration decreased from 8 ppm at 30 m to 2.5 ppm at 70 m. The modeled mean concentration in the separator experiment across all four distances was 2.6 ppm, compared to 3.8 ppm from observations.

Table 3.5: FAC2, MG, VG and NMSE for each experiment when evaluated against observed concentration for the separator experiment.

Distance (m)	FAC2	MG	VG	NMSE
30	0.54	1.96	4.74	3.43
45	0.76	1.27	1.43	0.84
60	0.95	0.98	1.07	0.19
70	0.93	0.84	1.20	0.28

Table 3.6: Fractional bias in maximum modeled concentration (CFD) for the separator experiment.

Distance (m)	Max Modeled Concentration (ppm)	Max Observed Concentration (ppm)	Fractional Bias (%)
30	38.65	57.02	-38
45	8.28	14.48	-54
60	8.52	7.25	16
70	9.32	9.71	-4

Table 3.7: Fractional bias in time-averaged modeled (CFD) concentration for the separator experiment.

Distance (m)	Mean Modeled Concentration (ppm)	Mean Observed Concentration (ppm)	Fractional Bias (%)
30	3.25	7.7	-82
45	2.31	3.37	-38
60	2.2	2.08	6
70	2.85	2.48	14

As per Hanna and Chang [45], FAC2 is the most robust model evaluation metric as it not influenced by outliers. The model performance is excellent with lowest FAC2 value of 0.54 at 30 m and as high as 0.95 and 0.93 for 60 m and 70 m, respectively. The MG value of 0.7 and 1.3 is well adhered to, except at 30 m where A high value for VG was also observed. However, the model does well with NMSE; having values within 4 at all the distances (Table 3.5). The high MG, VG and FB values at 30 m suggest a deviation between the model and the observations on all accounts. The same big underestimation is shown in other studies with the use of k-ϵ model [23]. The absolute fractional bias in the modeled maximum concentration at the distances modeled for the separator methane release stays between 4% and 54% (Table 3.6). The values are higher at smaller distances while dropping to 16% and 4% at 60 m and 70 m, respectively. The absolute fractional bias in the time-averaged modeled concentration shows a similar trend with higher values at 30 m and 45 m and drops down to 6% and 14% at 60 m and 70 m, respectively (Table 3.7). The metrics show the model performs better farther from the release point.

The NMB performs similarly, with the highest value of 0.58 at 30 m and dropping to 0.32, 0.06 and 0.15 at 45 m, 60 m and 70 m respectively (Table 3.8). The RMSE is 12 ppm at 30 m, decreasing to 7 ppm, 6.5 ppm and 6 ppm at 45 m, 60 m and 70 m, respectively. The R-value varied between 0.26 and 0.28, showing a weak linear relationship between model and observation (Table 3.8). However, the overlap coefficient is 0.83 and 0.88 at 45 m and 60 m, respectively, and performs weakly at 30 m and 70 m with the value of 0.62 and 0.48, respectively (Table 3.8).

Table 3.8: NMB, R-value, RMSE and overlap coefficient for each experiment when evaluated against observed concentration for the separator experiment.

Distance (m)	NMB	R-value	RMSE (ppm)	Overlap coefficient
30	-0.58	0.26	11.43	0.62
45	-0.32	0.29	7.55	0.83
60	0.06	0.29	6.56	0.88
70	0.15	0.29	6.17	0.48

3.3 Gaussian Plume Modeling Results

Gaussian plume modeling was performed for both the experiments— controlled release from the wellhead and release from the separator. Wind data was time-averaged for the experiment duration of 4-6 minutes for Gaussian modeling. The wind data and the weather conditions were used to determine the PGSC stability class and dispersion parameters from the look-up table (Appendix A). Stability classes for the experiments were either A or B (Appendix, Table A.1) in most of the cases. The results are mentioned in Tables 3.9 and 3.10.

Table 3.9: Fractional bias in time-averaged modeled (GP) concentration for the wellhead experiment.

Distance (m)	Mean Modeled Concentration (ppm)	Mean Observed Concentration (ppm)	Fractional Bias (%)
22	4.49	7.52	-50
33	1.93	2.82	-38
43	3.09	2.34	28
50	2.22	2.82	-24

Table 3.10: Fractional bias in time-averaged modeled (GP) concentration for the separator experiment.

Distance (m)	Mean Modeled Concentration (ppm)	Mean Observed Concentration (ppm)	Fractional Bias (%)
30	3.29	7.70	-80
45	3.60	3.37	-6
60	2.46	2.08	16
70	2.51	2.48	2

The absolute fractional bias in Gaussian plume modeled concentration stays within 50% for the wellhead experiment and under 80% for the separator experiment. Except for the two shortest distances i.e., 22 m and 30 m, the biases are within 40%. Gaussian model results shows an under

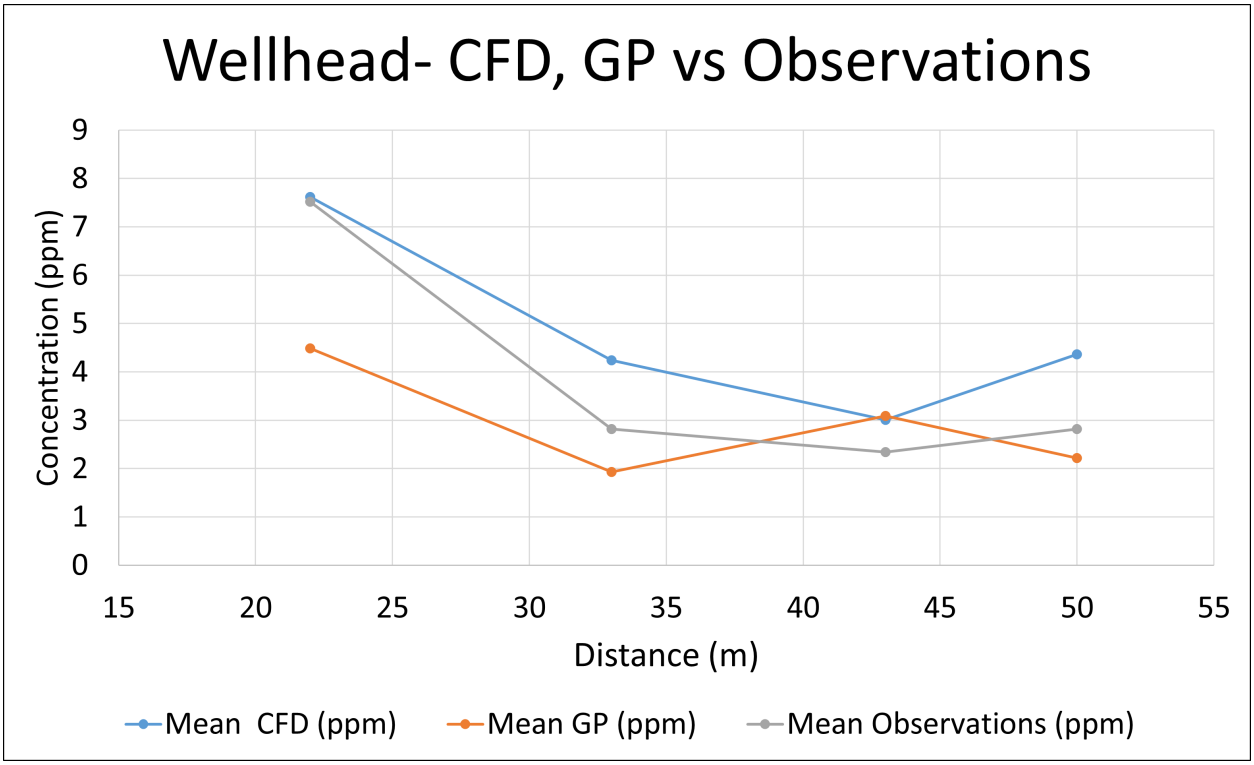

Figure 3.3: Time-averaged concentrations from the Gaussian model, the CFD model and the observations for the wellhead experiment.

prediction at shorter distances with FB values ranging from -50% to -80%. Figure 3.3 and 3.4 compare the time-averaged modeled concentrations from the Gaussian model, CFD model and the observations. The concentrations from the Gaussian plume model shows a decreasing trend in the both the experiments. Similarly, the fractional bias in modeled concentration decreases with distance for both the experiments, unlike the modeled concentrations from the CFD model.

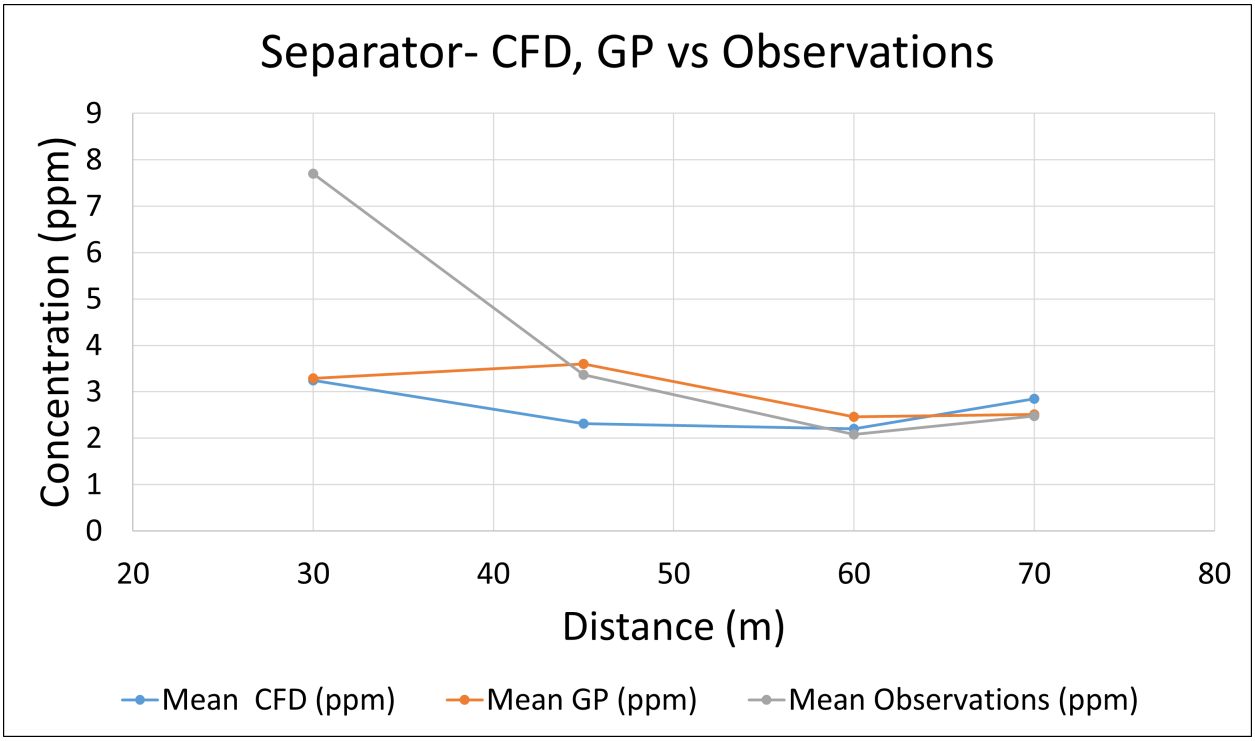

Figure 3.4: Time-averaged concentrations from the Gaussian model, the CFD model and the observations for the separator experiment.

3.4 Discussion

In this work, we studied the utility of CFD in modeling methane flows downwind of a methane release at a simulated oil and gas facility, similar to studies done by Toja et al. and Wen et al. [24,28,30,34] where CFD models were validated against field observations. We measured methane concentration downwind of controlled methane releases at fixed emission rates of 1.3 and 2.6 kg CH_4/h. A micro-portable greenhouse gas analyser (MGGA), a reference grade sensor, was used for the measurements. The controlled release experiments were done in an environment where only one emission point was active, and the point was precisely known; there was little uncertainty in the sensor's location, emission rate, and positioning relative to the emission point. Comparing measured to modeled concentrations downwind of these controlled emissions provides a good test of CONVERGE CFD to model external methane flows in similar environments.

3.4.1 CFD Model

Results from CONVERGE CFD were evaluated against the observations on multiple metrics used for evaluating CFD and Gaussian dispersion models against observations [45, 54]. The CFD model was evaluated on the metrics of FAC2, FB, NMSE, MG, VG and on additional parameters of NMB, R and RMSE. The CFD modeling results were compared against two controlled release experiments with different obstruction heights to test how the CFD results are affected by aerodynamic complexity. The first experiment released gas from a wellhead at 1.5 m above ground level and the second was from a separator with a release point of 2 m. The separator tanks are much larger and wider than the wellhead at the METEC facility. The model does very-well on FAC2 with all the experiments having a value greater than 0.5 in either experiment suggesting more than 50% of the modeled concentration within a value of 2 of the observations. The NMSE value of 4 is also satisfied in all the experiments.

However, the MG values are outside the limits of acceptability at 22 m, 30 m and 33 m (Section 2.7). Similarly, the VG values are outside the acceptability limits for 22 m, 30 m, 33 m and 50 m. The preferred FB values should be within $\pm$30%, however, the values are high for maximum modeled concentration at 30 m and 45 m for the separator experiment and 43 m and 50 m for the wellhead experiments. For the time averaged concentration, the FB values are out of the limits of acceptability for 33 m and 50 m for the wellhead experiment and 30 m and 45 m for the separator experiments. The CFD model in general underestimates the maximum methane concentrations in 6 of the 8 experiments. This was showcased in other studies with constant plume releases [24, 28]. The NMB, though, in all the cases stayed under $\sim$0.3 except for 30 m for the separator and 50 m for the wellhead experiment.

When simulated using the CFD model, we don't see the CFD model performing better for one equipment geometry type over the other. It is important to discuss the complexity of the separator and the wellhead since obstructions create complex wind speeds locally, including changes in turbulence, which in turn impact the dispersion of light gas species. In this evaluation, the CFD model showed satisfactory results compared to the observations with FB, MG and VG within the

limits of acceptability at some distances and out of the limits of acceptability at some distances while the NMSE and FAC2 stayed within the ranges of acceptability in both the wellhead and the separator experiment, irrespective of equipment complexity.

However, the CFD model is unable to capture the finer variations in the observations (Figure 3.1 and 3.2). This could be attributed to the RANS modeling approach along with the coarse grid used in the study. As studies have suggested that RANS formulation is inherently incapable of capturing unsteady effects, like intermittent separation, eddy generation, and transport [48]. LES approach is not a realizable solution since it requires high grid refinement leading to greater computational expense to properly resolve non-linear interactions at all scales to obtain meaningful turbulence statistics [59]. In order to capture the fluctuations in the modeled methane concentrations there is a need of hybrid RANS/LES methods- near-wall flow is modeled using a RANS approach coupled to an LES model away from the surface [60]. Since the CFD model is unable to capture the fine variations in the observations, we also compared the 3 s and 5 s (Figure B.1-4) moving average concentrations from CFD model and observations. However, the CFD model performance did not improve when evaluated with the averaged concentration.

A more robust evaluation of CFD model could not be done in this study due to computational and time restraints. Model evaluation done for Gaussian dispersion models and CFD models in previous studies considered huge datasets. In Prairie Grass Field experiment, 43 trials with multiple monitoring points in a variety of stability classes were conducted at five monitoring arcs (at 50, 100, 200, 400, and 800 m) [27]. The Kit Fox experiments [28] conducted downwind test of releases with 84-fast response monitors at 4 distances (25, 50, 100 and 225 m). A total of 52 release experiments were conducted split into 18 plume and 34 puff releases with 2 different arrays of obstacles. The mock urban setting test (MUST) field experiment consisted of 37 releases of tracer gas in an array of shipping containers as obstacles [61] with four sets of monitoring arrays at downwind distances of about 25, 60, 95, and 120 m.

While evaluating a CFD model in the studies [24, 28, 34] against these 3 experiments, only the maximum predicted tracer concentration at each monitoring points were evaluated against the

maximum observed concentration. Moreover, these tests were conducted at a very high release rate with resulting tracer concentrations in hundreds of ppm going up to over 1000 ppm in the Kit Fox experiment. All of the model evaluations in these studies [24, 28, 34] were done in space and none of the model evaluations of the predicted data was evaluated on a temporal scale. In two of the above studies, model evaluation were done at 25 m and 50 m, however, the CFD models were set-up for a larger domain with coarse grids and time-averaged model inputs. Although these studies serve as the basis for our work, the model evaluation metrics might not provide the best results in our case. The model evaluation in these existing studies are biased towards model performance in predicting maximum concentration which might diverge significantly from mean concentrations [24] with already high release rates. Our study has release rates typical of an O&G facility with much lower concentrations, hence, the model evaluation in our work is more sensitive to the model evaluation metrics.

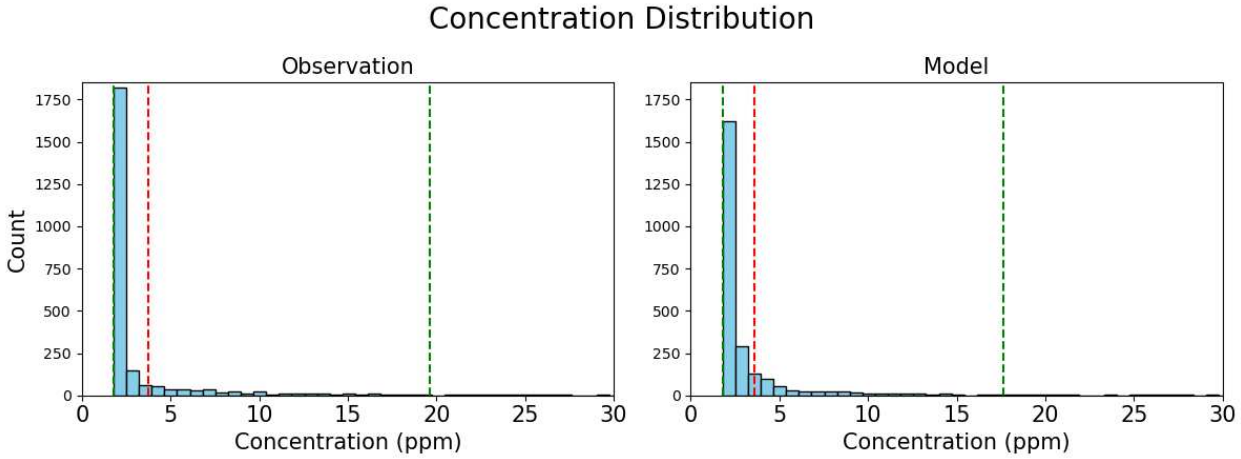

Figure 3.5: The concentration distribution of modeled (right) and observed (left) concentrations combined for all experiments. The dotted red lines show the mean concentration, and the green lines represent the 95% CI.

Now looking at the data using all 41 minutes of CFD simulation for all the experiments, the correlation coefficient (R-value) between the modeled and observed data is 0.29, suggesting a weak linear relationship (Figure 3.6), with an RMSE value of 6.16 ppm. We also evaluated the CFD model results with 3 s and 5 s moving averages to see if the R-value improves. The R

value improved slightly from 0.29 to 0.34, suggesting the model correlation does not improve greatly with moving average concentrations. Moreover, the model's effectiveness in estimating the concentration exceedances above the background concentration of 1.8 ppm was also evaluated. We found that the model can capture 57% of the exceedances (>1.8 ppm) but fails 15% of the time to predict the concentration above 1.8 ppm. Also there is a good overlap between modeled and observed concentrations overlap coefficient of 0.87 (Figure 3.5).

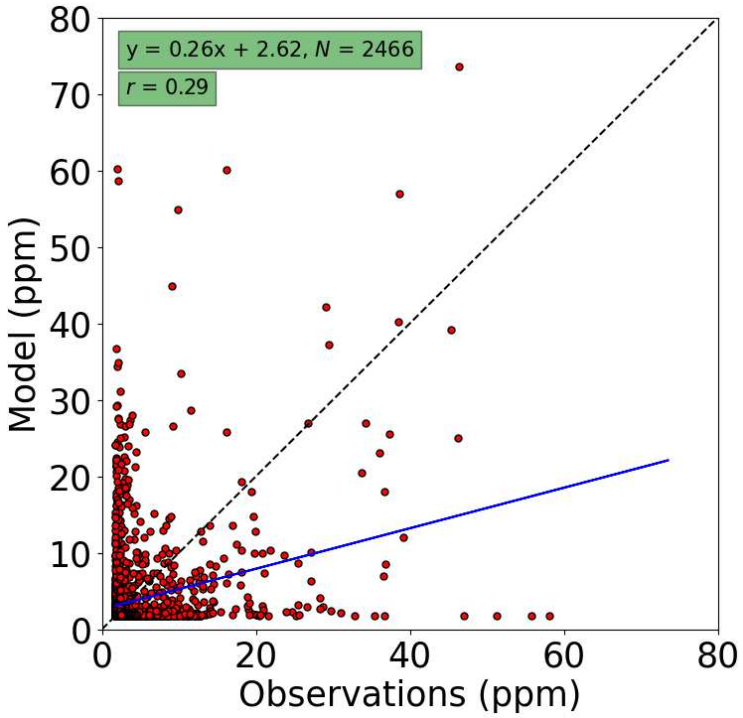

Figure 3.6: The modeled concentration plotted against the observed concentration with a linear fit in blue and a 1:1 line in black.

3.4.2 Gaussian Plume Model

Moreover, we also evaluated if CFD could outperform the simpler Gaussian plume (GP) model for both the wellhead and the separator experiment (Section 3.3). We find that the Gaussian plume model performs decently to estimate time-averaged mean concentration at fence-line distances. The bias in model concentration (GP) stayed under 80% for all the cases which is more than the

acceptability limit of $\pm 30\%$. Although there is no obstruction in consideration in GP modeling, the GP model performance is better for farther distances, i.e., for the separator experiments from 45-70 m and poorer at shorter distances where it massively underestimates methane concentrations. Figures 3.3 and 3.4 give a good idea of how the GP model is able to estimate the methane concentrations downwind of the methane emissions. The GP model biases are within 20% between 45-70 m for the separator experiment. For the wellhead experiments, GP model biases stay within 40% at farther distances with the maximum of -50% at 22 m. The under prediction could be a limitation of Gaussian dispersion models. Studies have shown that for unstable conditions (classes A and B) at short distances Gaussian models underestimate concentration and over predict at farther distances [62]. Mazzoldi et al. [24] have shown a similar trend when evaluating the Gaussian model ALOHA 5.4 with Prairie Grass experiments [27]. As discussed in the previous section a more robust analysis of Gaussian plume models was not done here due to limited experimental data. The metrics of MG, FAC2, VG and NMSE were employed with temporal data for the CFD model which is not possible for the Gaussian plume model. For the limited data of 8 points in our study the FAC2 value of 0.88 is excellent, though not surprising. More trials will help evaluate the model performance better.

3.4.3 CFD vs Gaussian Model

The biases in modeled concentrations for the Gaussian plume are similar to biases for the CFD model. Though unlike the CFD model, the absolute fractional bias in modeled concentration from Gaussian plume has a strong linear correlation with distance. The R-value is -0.79, suggesting that the model biases decrease with increasing distance for the Gaussian plume model. However, for CFD, the R-value for fractional biases in modeled mean concentration and distance is -0.32, showing a weaker correlation. The FB in mean modeled concentration was the only parameter to compare the CFD and Gaussian model. However, the model was evaluated on multiple metrics, hence we looked at the correlation coefficient of different evaluation metric with distance (Table 3.11). The correlation coefficient between the measurement distance and fractional bias in the

maximum concentration is 0.44. Similarly, the correlation coefficient between the NMB values and MG with modeled distance is 0.39 and -0.26, showing a weak linear relationship. However, the CFD model has a strong correlation with FAC2, VG and NMSE. We saw FAC2 increase with increasing distance while NMSE and VG decreased with increasing distance, indicating improved model performance with increasing distance. Conversely, FB and MG are indicative of mean bias and it does not correlate with distance. However, NMSE and VG are indicative of random scatter which strongly correlates with distance. Given our analysis, we can not say with certainty if the CFD model performance improves with increasing distances which is the case with our Gaussian plume model, albeit just on one parameter. In previous studies, little trends in CFD model performance with downwind distance were seen for the MUST and Kit Fox field experiments [28].

Table 3.11: Correlation coefficient of evaluation metrics with distance.

Evaluation Metric	R-value
FAC2	0.93
MG	-0.26
VG	-0.77
NMSE	-0.83
FB Max concentration (CFD)	0.44
FB Mean concentration (CFD)	-0.32
FB Mean concentration (GP)	-0.79

The results from CONVERGE CFD and the Gaussian plume modeling suggest that the CFD model was able to capture methane dispersion to a a modest degree based on the model evaluation metrics; however, the CFD simulations were too coarse to sufficiently capture turbulence and methane diffusion. A much finer grid with LES or DNS simulations could improve over the results achieved using RANS with a coarse grid because LES reproduces better the mean wind velocity and turbulence kinetic energy behind the obstructions [47, 63].

Despite a modest agreement between modeled and measured data, we found two significant shortcomings of the CFD model: the computational expense, and the technical expertise required

to run the model. The computational time of running CFD models for large domains, such as those used in this study, is very long compared to running the traditional Gaussian plume , with hours/days compared to minutes/seconds. The simulation time depends on domain discretization, i.e., the grid size, length of time, number of steps per second the model physics, solution algorithms and system approximations [24, 28, 34]. The grid size in the simulations was coarse to keep the simulation time between 6-14 hours. The simulation times will further increase if the grids are made finer or LES or other turbulence models are applied.

There are more requirements to run CFD simulations than running a Gaussian plume model. Computer aided designs (CAD) are required for all the equipment in the simulation domain. The CAD models must be prepared in a model-ready format. Like the simple models, wind data are required, but further modeling is required to generate wind data at interval heights between 0-15 meters. In addition, simulation parameters, boundary conditions, and initial conditions must be set to run CFD simulations.

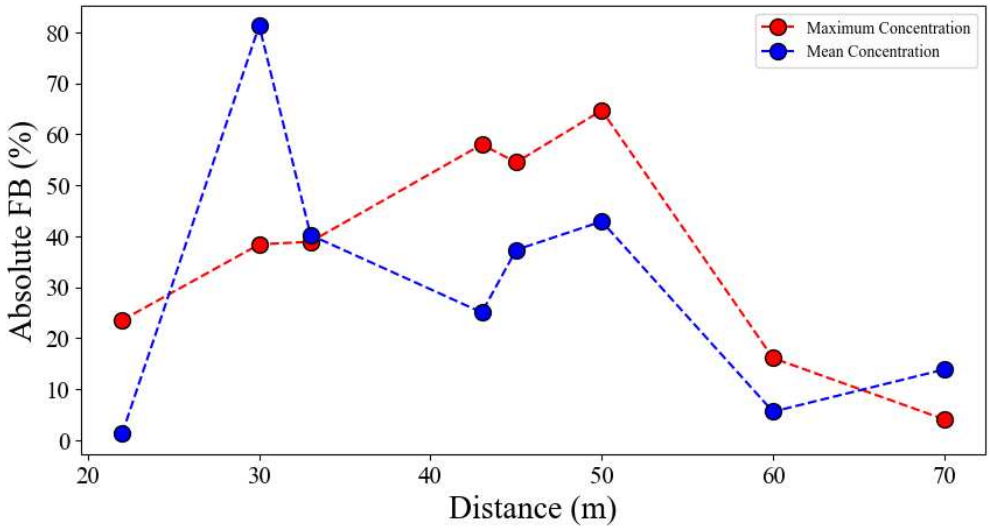

Figure 3.7: Absolute fractional bias in the modeled mean and maximum concentrations at downwind observations under 70 m.

Chapter 4

Conclusions

4.1 Summary

This study aims to investigate if methane concentrations downwind of a release can be modeled using a CFD model. To investigate the hypothesis, CFD simulations using CONVERGE CFD were run based on controlled methane release experiments conducted at CSU's METEC facility in Fort Collins, Colorado. The CFD simulations mimicked two controlled release experiments on 21st March 2024 between 9-11 AM and on 11th July 2024 between 1-3 PM— controlled release of 1.3 kg CH_4/h from a separator, and controlled release of 2.6 kg CH_4/h from a wellhead, respectively. The measurements were done using a reference grade micro-portable greenhouse gas analyzer (MGGA). Methane measurements were done at 4 distances ranging between 20-70 meters from the release point on these two days. The controlled release experiments were done in an environment where only one emission point was active with no obstructions between the source and measurement points, and the point was precisely known; there was little uncertainty in the sensor's location, emission rate, and positioning relative to the emission point. The CFD model results are then evaluated against the observational data from the field on the metric of fractional bias, FAC2, fractional bias, and geometric mean bias, normalize mean square error and geometric variance based on previous studies [45, 54, 55] and used in several studies to evaluate dispersion models [24, 34]. The evaluation metrics used in this study are biased towards evaluating maximum concentrations from dispersion models not time-averaged concentrations [24]. In our work, we evaluated the CFD model performance on spatial as well as temporal scale. Moreover, due to limited experimental data we also used some other model evaluation metrics like normalized mean bias, correlation coefficient, overlap coefficient and root mean square error. Further, to evaluate if the model performs better than a simple dispersion model, Gaussian plume modeling was also done in the study. Results from the Gaussian plume model were evaluated against the observed data

form the controlled methane release experiments. To evaluate the Gaussian plume model against the observations, the field data was averaged for observed duration of 4-6 minutes. The overall CFD model performance, the model performance with equipment complexity and the performance of the Gaussian plume model were analyzed.

4.2 Specific Conclusions

The CFD model shows a modest performance while evaluated on the basis of multiple evaluation metrics. The metrics fall mostly in the range of acceptability. The FB in the modeled maximum concentration stays in the range of -0.58 to 0.65, which is larger than the $\pm 30\%$ acceptability limit for FB. However, existing literature [45] with CFD model evaluation against research grade experiments [27, 28, 61] show a similar range of FB values. Values for FAC2, which is a robust measure of model performance, stayed above 0.54 in all the experiments. For NMSE, values stayed under the suggested limit of 4 and rest of the performance metrics were within the ranges found in literature with model evaluation against research grade experiments [27, 28, 61]. The mean modeled concentrations from CFD and GP model results were evaluated on the metric of fractional bias. While the FB values are modest for both the models, CFD and GP predict the mean concentration with $\sim$ ±80% bias. However, we find that GP modeled methane concentration is strongly correlated to distance, unlike the modeled concentration from a CFD model with R-value of -0.79 and -0.32 respectively. The CFD model, on the other hand, provides methane concentration data at 1 Hz frequency and is able to capture the observed maximum concentrations to a good degree (under 65%, Figure 3.7) in all cases which can't be obtained through the Gaussian plume model. Results suggest that CFD modeling approaches can be used to generate representative time-averaged (4–6-minute average in our study) concentrations at the fence-line of $\sim$30 m for oil and gas production equipment (Figure 3.5) with modest success. However, results from the CONVERGE CFD model at shorter distances could be improved with good input data, optimized parameters with finer grid and a better turbulence model like LES and DNS [47, 63]. From this limited comparison (only two cases studied), there does not appear to be bias caused by the aero-

dynamic complexity of the emission point. The CFD model does not perform better selectively for the wellhead or the separator experiments than the GP approach despite one being more complex than the other. While the CFD modeling results are satisfactory, we suggest that the demands of running the CFD (computational time and technical expertise) mean that CFD is unlikely to replace the current atmospheric dispersion model when rapid responses are required until the models are simplified or computer-runs much faster. However, this work, along with existing literature, make a strong case for CFD to be used in designing, developing and studying O&G facilities, not only for hazardous study, but for the detection and quantification of methane.

4.3 Future Work

In this work, we have used a CFD tool to model methane concentrations downwind of a release at pseudo oil and gas facility. The investigations used modeling tools and evaluated the results using measurements. While a good amount of time and effort was spent in this study, there are some recommendations for future work to improve the technique.

The wind data used in the study is collected using an anemometer located at the fringe of the METEC facility (Figure 2.3). The wind data from this anemometer might not be representative of the wind data at the measurement point or the point of methane release. Future studies should be done with the anemometer co-located with the emission source to have more representative wind data for CFD modeling.

The wind modeling done in this work used a simple model (Equation 2.1) to model the wind speed from ground to 15 m height. However, this was done assuming an unobstructed wind profile at the point of release. As mentioned and can be seen in (Figure 2.3), for the cases modeled in this work, the wind goes through other additional METEC equipment/structures, adding to turbulence. In the future, wind modeling should be done using a better wind model which takes the obstructions into upwind consideration— leading to an improved wind data for CFD modeling.

In this work, we have considered two equipment— a smaller and less complex wellhead and a set of separator tanks. There are other release points at the METEC facility (Figure 2.1), situated

on other pads. Notably, there are a set of tanks which are the largest equipment at the facility. Future studies should consider more complex release scenarios, such as from tanks that are both taller and wider than the separators and wellhead investigated in this study.

Last but not the least, every CFD model has differences in how the model is designed, even when the underlying principles are the same. A similar model set-up in two different models could provide different sets of results. Model parameters are critically important; hence, additional sensitivity simulations must be carried out to study the impact of underlying model physics, physical parameter values and other parameters on simulation results [30].

Bibliography

[1] U.S. Environmental Protection Agency (EPA). Global greenhouse gas overview. https://www.epa.gov/ghgemissions/global-greenhouse-gas-overview, 2024. Accessed: Oct 29, 2024.

[2] U.S. Environmental Protection Agency. Inventory of US greenhouse gas emissions and sinks: 1990-2020 (EPA, 2024). https://www.epa.gov/ghgemissions/inventory-us-greenhouse-gas-emissions-and-sinks, 2024. Accessed: Oct 29, 2024.

[3] U.S. Energy Information Administration (EIA). Natural gas and the environment. https://www.eia.gov/energyexplained/natural-gas/natural-gas-and-the-environment.php, 2025. Accessed: Jan 17, 2025.

[4] Chiemezie Ilonze, Ethan Emerson, Aidan Duggan, and Daniel Zimmerle. Assessing the progress of the performance of continuous monitoring solutions under a single-blind controlled testing protocol. *Environmental Science & Technology*, 58:10941–10955, Jun 2024.

[5] C. Bell, C. Ilonze, A. Duggan, and D. Zimmerle. Performance of continuous emission monitoring solutions under a single-blind controlled testing protocol. *Environmental Science & Technology*, 57(14):5794–5805, Apr 2023.

[6] ABB. Off-Axis Integrated Cavity Output Spectroscopy (OA-ICOS) microportable analyzers GLA131 series. https://new.abb.com/products/measurement-products/analytical/laser-gas-analyzers/laser-analyzers/lgr-icos-portable-analyzers/lgr-icos-microportable-analyzers-gla131-series, 2025. Accessed: Feb 12, 2025.

[7] Cavity Ring-Down Spectroscopy | Picarro. https://www.picarro.com/company/technology/crds, 2024. Accessed: Oct 30, 2024.

[8] P. Mahbub, A. Noori, J. S. Parry, J. Davis, A. Lucieer, and M. Macka. Continuous and real-time indoor and outdoor methane sensing with portable optical sensor using rapidly pulsed IR LEDs. *Talanta*, 218:121144, 2020.

[9] S.N. Riddick, D.L. Mauzerall, M. Celia, G. Allen, J. Pitt, M. Kang, and J.C. Riddick. The calibration and deployment of a low-cost methane sensor. *Atmospheric Environment*, 230:117440, 2020.

[10] S. N. Riddick, D. L. Mauzerall, M. A. Celia, M. Kang, and K. Bandilla. Variability observed over time in methane emissions from abandoned oil and gas wells. *International Journal of Greenhouse Gas Control*, 100:103116, 2020.

[11] D. Bastviken, J. Nygren, J. Schenk, R. Parellada Massana, and N. T. Duc. Technical note: Facilitating the use of low-cost methane sensors in flux chambers – calibration, data processing, and an open-source make-it-yourself logger. *Biogeosciences*, 17(13):3659–3667, 2020.

[12] W. Eugster and G. W. Kling. Performance of a low-cost methane sensor for ambient concentration measurements in preliminary studies. *Atmospheric Measurement Techniques*, 5(8):1925–1934, 2012.

[13] R. E. Day, E. Emerson, C. Bell, and D. Zimmerle. Point sensor networks struggle to detect and quantify short controlled releases at oil and gas sites. *Sensors*, 24(8):2419, 2024.

[14] C. Bell and D. Zimmerle. METEC controlled test protocol: Continuous monitoring emission detection and quantification. Sep 2020.

[15] M. Mbua, S. N. Riddick, E. Kiplimo, and D. Zimmerle. Evaluating the accuracy of downwind methods for quantifying point source emissions. *EGUsphere*, 2024.

[16] M. Jia, W. Daniels, and D. Hammerling. Comparison of the Gaussian plume and puff atmospheric dispersion models on oil and gas facilities. *Energy*, Jan 2023.

[17] U.S. Department of Health, Human Services, Centers for Disease Control, and Prevention. Significant dust dispersion models for mining operations. *National Institute for Occupational Safety and Health*, Sep 2005.

[18] S. N. Riddick, M. Mbua, J. C. Riddick, C. Houlihan, A. L. Hodshire, and D. J. Zimmerle. A cautionary report of calculating methane emissions using low-cost fence-line sensors. *Elementa: Science of the Anthropocene*, 10(1):00021, May 2022.

[19] Glenn Research Center | NASA. Navier-Stokes equation. https://www1.grc.nasa.gov/beginners-guide-to-aeronautics/navier-strokes-equation/. Accessed: Sep 18, 2024.

[20] R. L. Petersen. Effect of homogeneous and heterogeneous surface roughness on heavier-than-air gas dispersion. *Journal of Wind Engineering and Industrial Aerodynamics*, 36:643–652, Jan 1990.

[21] H. Wang, B. Liu, X. Liu, C. Lu, J. Deng, and Z. You. Dispersion of CO_2 released from buried high-pressure pipeline over complex terrain. *Environmental Science and Pollution Research*, 28(6):6635–6648, Feb 2021.

[22] J. Xing, Z. Liu, P. Huang, C. Feng, Y. Zhou, D. Zhang, and F. Wang. Experimental and numerical study of the dispersion of CO_2 plume. *Journal of Hazardous Materials*, 256–257:40–48, Jul 2013.

[23] S. Sklavounos and F. Rigas. Validation of turbulence models in heavy gas dispersion over obstacles. *Journal of Hazardous Materials*, 108(1):9–20, Apr 2004.

[24] A. Mazzoldi, T. Hill, and J. Colls. CFD and Gaussian atmospheric dispersion models: A comparison for leak from CO_2 transportation and storage facilities. *Atmospheric Environment*, 42(34):8046–8054, 2008.

[25] Fluidyn-Panache - CFD software for air quality and gas dispersion. https://www.fluidyn.com/fluidyn-consultancy-software-cfd-multiphysics-11/fluidyn-panache/, 2025. Accessed: Mar 17, 2025.

[26] US EPA. ALOHA software. https://www.epa.gov/cameo/aloha-software, 2025. Accessed: Mar 17, 2025.

[27] Atmospheric Analysis Laboratory. *Project Prairie Grass, a field program in diffusion: Volume 1*. Geophysical Research Papers, US Air Force Cambridge Research Center, Bedford, Massachusetts, 1958.

[28] S. R. Hanna and J. C. Chang. Use of the Kit Fox field data to analyze dense gas dispersion modeling issues. *Atmospheric Environment*, 35(13):2231–2242, May 2001.

[29] A. M. Schleder and M. R. Martins. Experimental data and CFD performance for CO_2 cloud dispersion analysis. *Journal of Loss Prevention in the Process Industries*, 43:688–699, Sep 2016.

[30] F. Toja-Silva, J. Chen, S. Hachinger, and F. Hase. CFD simulation of CO_2 dispersion from urban thermal power plant: Analysis of turbulent schmidt number and comparison with Gaussian plume model and measurements. *Journal of Wind Engineering and Industrial Aerodynamics*, 169:177–193, Oct 2017.

[31] OpenFOAM. https://www.openfoam.com/, 2025. Accessed: Mar 17, 2025.

[32] W. Tan, C. Li, K. Wang, G. Zhu, Y. Wang, and L. Liu. Dispersion of CO_2 plume in street canyons. *Process Safety and Environmental Protection*, 116:235–242, 2018.

[33] C. J. Wareing, M. Fairweather, S. A. E. G. Falle, and R. M. Woolley. Validation of a model of gas and dense phase CO_2 jet releases for carbon capture and storage application. *International Journal of Greenhouse Gas Control*, 20:254–271, Jan 2014.

[34] J. Wen, A. Heidari, B. Xu, and H. Jie. Dispersion of CO_2 from vertical vent and horizontal releases—A numerical study. *Proceedings of the Institution of Mechanical Engineers, Part E: Journal of Process Mechanical Engineering*, 227(2):125–139, 2013.

[35] J. X. Wen, P. Le Fur, H. Jie, and C. M. R. Vendra. Further development and validation of CO2FOAM for the atmospheric dispersion of accidental releases from CO_2 pipelines. *International Journal of Greenhouse Gas Control*, 52:293–304, 2016.

[36] B. Liu, X. Liu, C. Lu, A. Godbole, G. Michal, and A. K. Tieu. Computational fluid dynamics simulation of CO_2 dispersion in a complex environment. *Journal of Loss Prevention in the Process Industries*, 40:419–432, Mar 2016.

[37] Ansys Fluent | Fluid simulation software. https://www.ansys.com/products/fluids/ansys-fluent, 2025. Accessed: Mar 17, 2025.

[38] P. Joshi, P. Bikkina, and Q. Wang. Consequence analysis of accidental release of supercritical CO_2 from high-pressure pipelines. *International Journal of Greenhouse Gas Control*, 55:166–176, Dec 2016.

[39] Colorado State University. METEC | Colorado State University. https://metec.colostate.edu/, 2024. Accessed: Sep 02, 2024.

[40] S. N. Riddick, M. Mbua, J. C. Riddick, C. Houlihan, A. L. Hodshire, and D. J. Zimmerle. Uncertainty quantification of methods used to measure methane emissions of 1 g CH_4 h^{-1}. *Sensors*, 23(22), 2023.

[41] Microportable Greenhouse Gas Analyser, (MGGA). https://www.sol-ma.net/wp-content/uploads/2018/07/DS_LGR-ICOS_MGGA-EN-Rev.-C.pdf, 2018. Accessed: Sep 19, 2024.

[42] R. M. Young Company. Wind monitor - propeller vane. https://www.youngusa.com/product/wind-monitor/. Accessed: Feb 14, 2025.

[43] J. H. Seinfeld and S. N. Pandis. *Atmospheric Chemistry and Physics: From Air Pollution to Climate Change*. J. Wiley, Hoboken, N.J, 2nd edition, 2006.

[44] CONVERGE CFD Software. CONVERGE CFD. https://convergecfd.com. Accessed: Jan 17, 2025.

[45] S. R. Hanna, O. R. Hansen, and S. Dharmavaram. FLACS CFD air quality model performance evaluation with Kit Fox, MUST, Prairie Grass, and EMU observations. *Atmospheric Environment*, 38(28):4675–4687, Sep 2004.

[46] C. Caron, P. Lauret, and A. Bastide. Machine learning to speed up CFD engineering simulations for built environments: A review. *Building and Environment*, 267:112229, Jan 2025.

[47] T. Nozu and T. Tamura. LES of turbulent wind and gas dispersion in a city. *Journal of Wind Engineering and Industrial Aerodynamics*, 104–106:492–499, May 2012.

[48] J. Sumner, C. S. Watters, and C. Masson. CFD in wind energy: The virtual, multiscale wind tunnel. *Energies*, 3(5):989–1013, May 2010.

[49] G. Patnaik, J. P. Boris, T. R. Young, and F. F. Grinstein. Large scale urban contaminant transport simulations with Miles. *Journal of Fluids Engineering*, 129(12):1524–1532, Apr 2007.

[50] CONVERGE CFD. Converge 3.0 manual. https://convergecfd.com. Accessed: Jan 17, 2025.

[51] Autodesk. Autodesk fusion | 3D CAD, CAM, CAE, and PCB cloud-based software. https://www.autodesk.com/products/fusion-360, 2025. Accessed: Jan 17, 2025.

[52] A. Hockett, G. Hampson, and A. J. Marchese. Development and validation of a reduced chemical kinetic mechanism for CFD simulations of natural gas/diesel dual-fuel engines. *Energy Fuels*, 30(3):2414–2427, 2016.

[53] S. K. Gupta and M. Mittal. Analysis of cycle-to-cycle combustion variations in a spark-ignition engine operating under various biogas compositions. *Energy Fuels*, 33(12):12421–12430, 2019.

[54] J. C. Weil, R. I. Sykes, and A. Venkatram. Evaluating air-quality models: Review and outlook. *Journal of Applied Meteorology and Climatology*, 31(10):1121–1145, 1992.

[55] S. R. Hanna, J. C. Chang, and D. G. Strimaitis. Hazardous gas model evaluation with field observations. *Atmospheric Environment*, 27(15):2265–2285, 1993.

[56] J. C. Chang and S. R. Hanna. Air quality model performance evaluation. *Meteorology and Atmospheric Physics*, 87(1):167–196, Sep 2004.

[57] G. P. Brasseur and D. J. Jacob. *Modeling of Atmospheric Chemistry*. Cambridge University Press, 1st edition, 2017.

[58] X. Liu, A. Godbole, C. Lu, G. Michal, and V. Linton. Investigation of the consequence of high-pressure CO_2 pipeline failure through experimental and numerical studies. *Applied Energy*, 250:32–47, Sep 2019.

[59] N. Wood. Wind flow over complex terrain: A historical perspective and the prospect for Large-Eddy Modelling. *Boundary-Layer Meteorology*, 96(1):11–32, 2000.

[60] A. Bechmann and N. Sørensen. Hybrid RANS/LES method for wind flow over complex terrain. *Wind Energy: An International Journal for Progress and Applications in Wind Power Conversion Technology*, 13(1):36–50, 2010.

[61] Christopher A Biltoft. Customer report for mock urban setting test. *U.S. Army Developmental Test Command*, (8-CO):160–000, 2001.

[62] S. Dharmavaram, S. R. Hanna, and O. R. Hansen. Consequence analysis using a CFD model for industrial sites. *Process Safety Progress*, 24(4):316–272, 2005.

[63] Y. Tominaga, A. Mochida, S. Murakami, and S. Sawaki. Comparison of various revised k–ϵ models and LES applied to flow around a high-rise building model with 1:1:2 shape placed within the surface boundary layer. *Journal of Wind Engineering and Industrial Aerodynamics*, 96(4):389–411, Apr 2008.

Appendix A

Gaussian Plume Model

Table A.1: Pasquill-Gifford atmospheric stability class look-up table.

Stability Class	Day			Night	
WS (m/s)	Strong	Moderate	Light	Overcast	Clear
2	A	A	B		
3	B	B	C	E	F
4	B	C	C	D	E
5	C	C	D	D	D
6	C	D	D	D	D

Table A.2: Parameters (a and b) needed to calculate Pasquill-Gifford σ_z.

		$\sigma_z = ax^b$ (x in km)	
Pasquill Stability Category	x (km)	a	b
A^*	< 0.10	122.800	0.94470
	0.10-0.15	158.080	1.05420
	0.16-0.20	170.220	1.09320
	0.21-0.25	179.520	1.12620
	0.26-0.30	217.410	1.26440
	0.31-0.40	258.890	1.40940
	0.41-0.50	346.750	1.72830
	0.51-3.11	453.850	2.11660
	> 3.11	**	**
B^*	< 0.20	90.673	0.93198
	0.21-0.40	98.483	0.98332
	>0.40	109.300	1.09710
C^*	All	61.141	0.91456
D	< 0.30	34.459	0.86974
	0.31-1.00	32.093	0.81066
	1.01-3.00	32.093	0.64403
	3.01-10.00	33.504	0.60486
	10.01-30.00	44.053	0.51179
E	< 0.10	24.260	0.83660
	0.10-0.30	23.331	0.81956
	0.31-1.00	21.331	0.81956
	1.01-2.00	21.628	0.63077
	2.01-4.00	22.534	0.57154
	4.01-10.00	24.703	0.50527
	10.01-20.00	26.970	0.46713
	20.01-40.00	35.420	0.37615
	> 40.00	47.618	0.29592
F	< 0.20	15.209	0.81558
	0.21-0.70	14.457	0.78407
	0.71-1.00	13.953	0.68465
	1.01-2.00	13.953	0.63227
	2.01-3.00	14.823	0.54503
	3.01-7.00	16.287	0.46490
	7.01-15.00	17.836	0.41507
	15.01-30.00	22.651	0.32681
	30.01-60.00	27.074	0.27436
	>60.00	34.219	0.21716

* If σ_z exceed 5000 m, $\sigma_z = 5000$ m, ** $\sigma_z = 5000$ m.

Table A.3: Parameters (c and d) needed to calculate Pasquill-Gifford σ_y.

$\sigma_y = 465.11628(x)tan(\theta), \theta = 0.017453293[c-(d)ln(x)]$		
Pasquill Stability Category	c	d
A	24.167	2.5334
B	18.333	1.8096
C	12.500	1.0857
D	8.3330	0.72382
E	6.2500	0.54287
F	4.1667	0.36191

where σ_y is in meters and x is in kilometers

Appendix B

CFD Model vs Observations

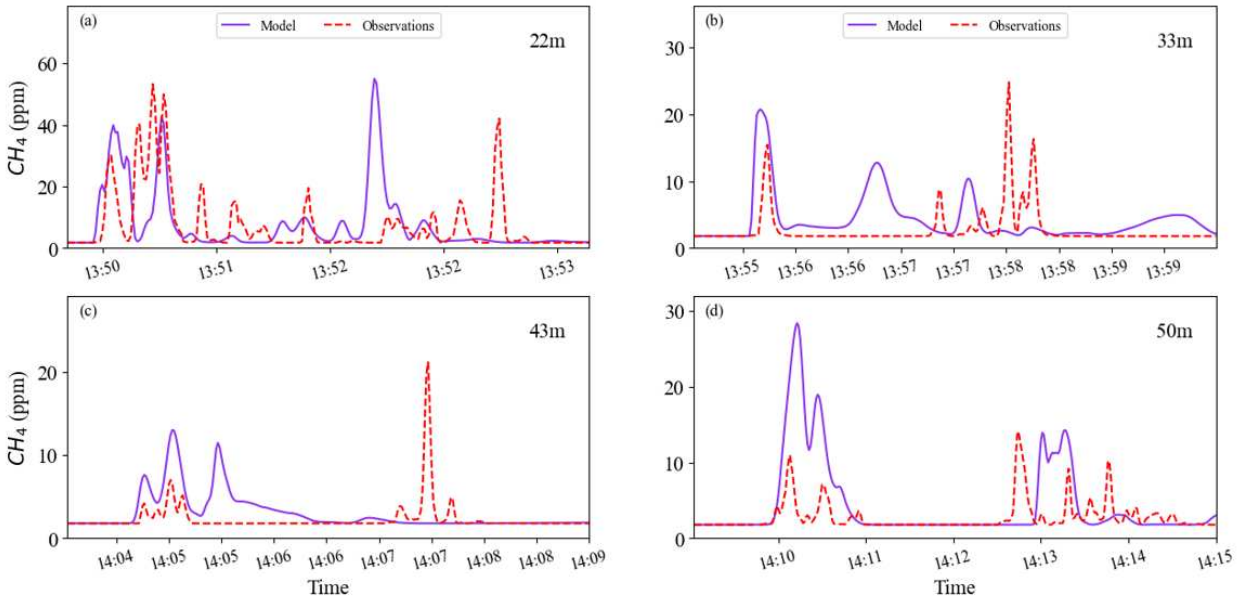

Figure B.1: Modeled methane concentration (3 s moving average) plotted against observations (3 s moving average) for release from the wellhead on 11th July 2024. The y-axis shows the methane concentration with time displayed in hours and minutes (also, y-axes have different bounds in the plots a-d).

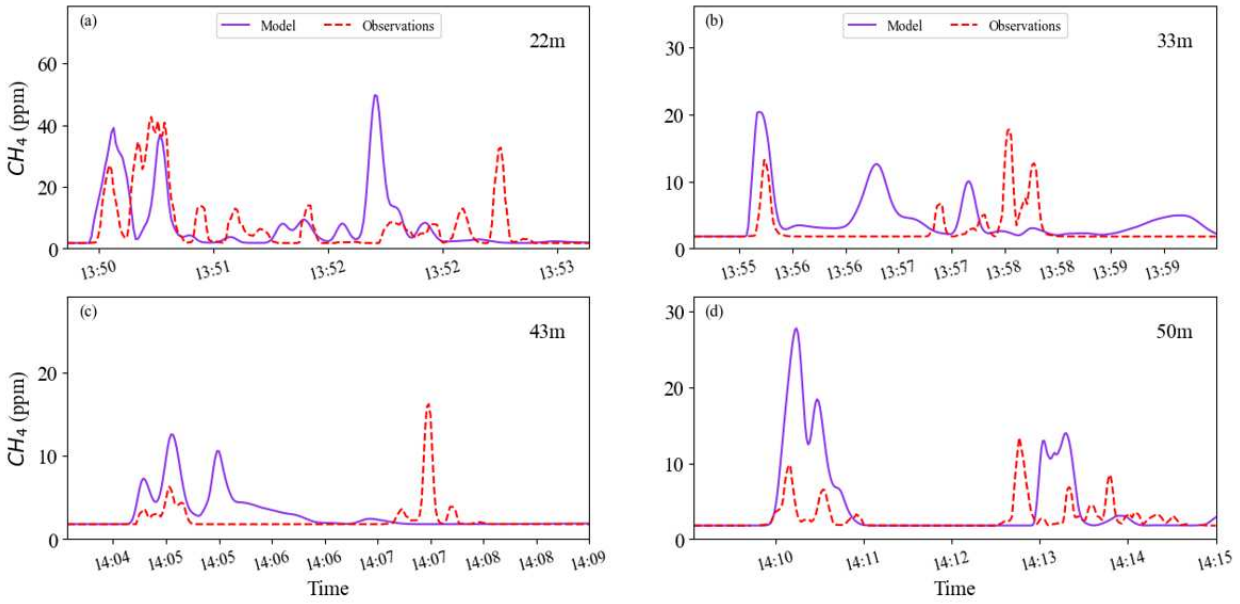

Figure B.2: Modeled methane concentration (5 s moving average) plotted against observations (5 s moving average) for release from the wellhead on 11th July 2024. The y-axis shows the methane concentration with time displayed in hours and minutes (also, y-axes have different bounds in the plots a-d).

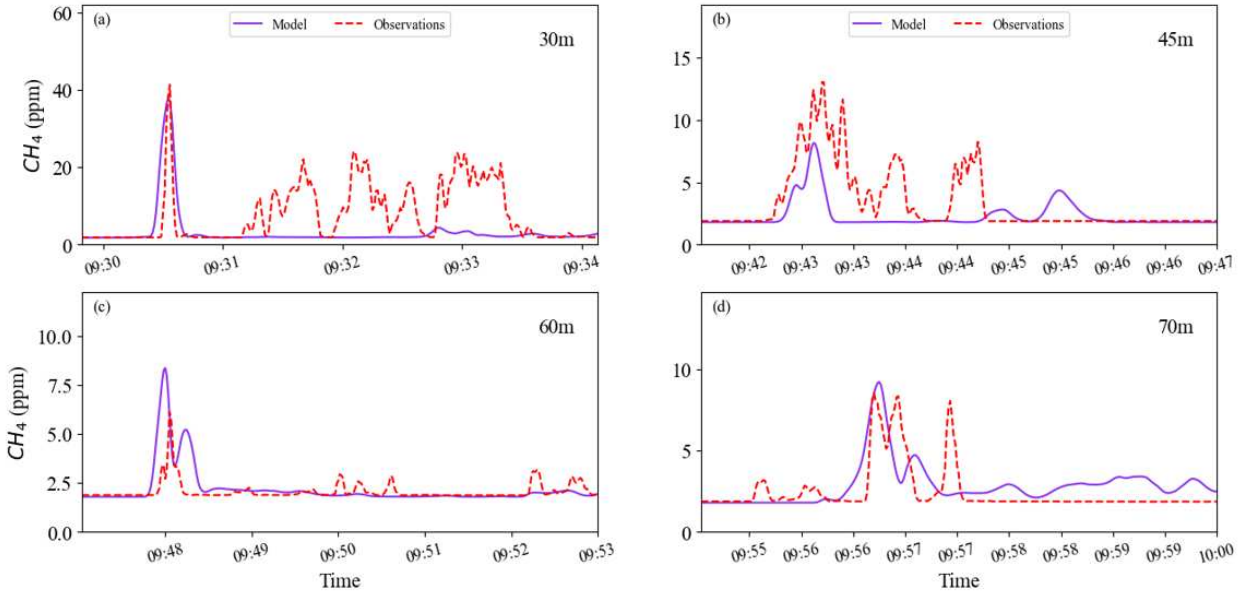

Figure B.3: Modeled methane concentration (3 s moving average) plotted against observations (3 s moving average) for release from the separator on March 21st 2024. The y-axis shows the methane concentration with time displayed in hours and minutes (also, y-axes have different bounds in the plots a-d).

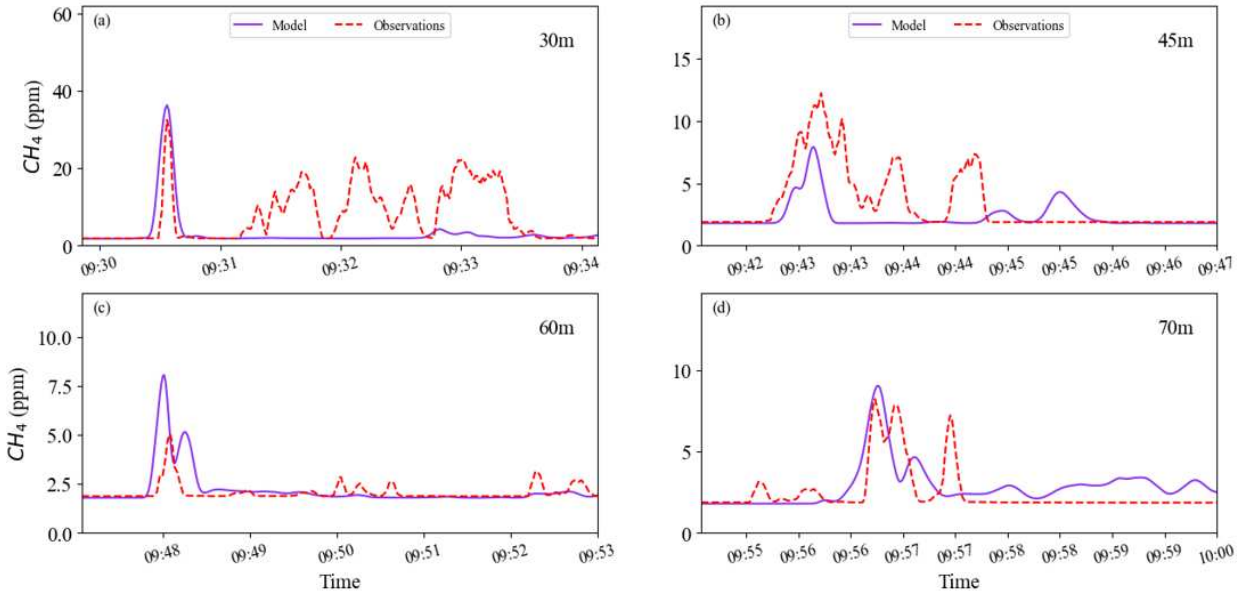

Figure B.4: Modeled methane concentration (5 s moving average) plotted against observations (5 s moving average) for release from the separator on March 21st 2024. The y-axis shows the methane concentration with time displayed in hours and minutes (also, y-axes have different bounds in the plots a-d).